

# THE SUPERSYMMETRIC PARTICLE SPECTRUM

V. Barger, M.S. Berger, and P. Ohmann

*Physics Department, University of Wisconsin, Madison, WI 53706, USA*

## Abstract

We examine the spectrum of supersymmetric particles predicted by grand unified theoretical (GUT) models where the electroweak symmetry breaking is accomplished radiatively. We evolve the soft supersymmetry breaking parameters according to the renormalization group equations (RGE). The minimization of the Higgs potential is conveniently described by means of tadpole diagrams. We present complete one-loop expressions for these minimization conditions, including contributions from the matter and the gauge sectors. We concentrate on the low  $\tan\beta$  fixed point region (that provides a natural explanation of a large top quark mass) for which we find solutions to the RGE satisfying both experimental bounds and fine-tuning criteria. We also find that the constraint from the consideration of the lightest supersymmetric particle as the dark matter of the universe is accommodated in much of parameter space where the lightest neutralino is predominantly gaugino. The supersymmetric mass spectrum displays correlations that are model-independent over much of the GUT parameter space.

## 1 Introduction

Why should one be interested in supersymmetry? Until recently, the reasons have been principally theoretical. Supersymmetry (SUSY) is a beautiful extension of the Poincaré symmetry with new dimensions of space and time that explain the existence of fermions[1]. It solves the hierarchy problem of widely separated electroweak and grand unified scales through cancellations among diagrams that give quadratically

divergent Higgs boson mass corrections. Moreover supersymmetry may be a necessary consequence of string theory.

The recent upswing in interest in supersymmetry derives from high precision measurements of Standard Model (SM) parameters at LEP. Renormalization group evolution with minimal SM particle content of the SU(3), SU(2), and U(1) couplings from  $Q^2 = M_Z^2$  do not converge at a single high scale, in contradiction with the prediction of the SU(5) grand unified theory (GUT). However, with the minimal particle content of supersymmetry included, the evolution is in excellent agreement with LEP data and suggests a grand unified scale at  $M_G \simeq 2 \times 10^{16}$  GeV and effective SUSY mass scale within the range  $M_Z < M_{SUSY} < 1$  TeV[2]. Encouraged by this success, the evolution of Yukawa couplings is also being vigorously pursued, with Yukawa unification constraints such as  $\lambda_b = \lambda_\tau$  at the GUT scale[3]. While the unification of gauge and Yukawa couplings is an extremely attractive feature, the existence of supersymmetry will only be confirmed when new particle states are seen directly and the associated R-parity conservation or violation is tested in the production and decays of these supersymmetric particles.

The idea of a radiative breaking of the electroweak symmetry is an old but still popular one[4]–[13]. It is very attractive to explain the breaking of the electroweak symmetry through large logarithms between the Planck scale and the weak scale[5]. For the radiative corrections to be strong enough to drive a Higgs boson mass-squared parameter negative (thus breaking the electroweak symmetry), a Yukawa coupling of that Higgs boson must be large at the GUT scale. With the top quark mass large

( $m_t > 100$  GeV), the SUSY GUT unification can naturally explain the origin of the electroweak scale. A heavy top is required to drive one of the soft-supersymmetry breaking parameters (a Higgs doublet mass) negative. Today we know the top quark mass is large and that the top has a large Yukawa coupling. There is a relationship between the electroweak scale and the top quark Yukawa coupling through the RGEs; consequently the radiative symmetry breaking mechanism has important consequences for the supersymmetric particle spectrum. Indeed a large top Yukawa coupling is the motivation for the fixed point solutions[14] advocated recently in the context of GUT theories[15]–[18]. These solutions predict a linear relationship between  $m_t$  and  $\sin \beta$ , given further constraints on the SUSY particle spectrum.

There are at least two other motivations for supersymmetry. In the context of SUSY GUTs, the grand unification scale is raised sufficiently high to suppress proton decay to experimentally acceptable levels, when an additional R-parity symmetry is invoked. R-parity symmetry has an important consequence, providing the second additional motivation for supersymmetry – it implies that the lightest supersymmetric particle (LSP) is stable. It is now generally believed that baryonic matter is insufficient to make up the total gravitationally interacting matter of the universe. The LSP provides a natural candidate for the (cold) dark matter of the universe, since the LSP is forbidden to decay into baryons by R-parity conservation.

The greatest dilemma for supersymmetry is the unknown mechanism for supersymmetry breaking. Since no supersymmetric partners of the known particles have been observed, one must not only explain why supersymmetry is broken, but also why

it is broken in such a way that (almost) all of the supersymmetric partners are heavier than the known particles. Typically one skirts the issue of the exact mechanism of supersymmetry breaking, and parametrizes one's ignorance by introducing soft-supersymmetry breaking parameters which characterize the scale of the masses of the supersymmetric particles. In the context of certain models (minimal supergravity, no-scale supergravity, superstring-inspired, etc.) there are relations between these parameters at the GUT scale that appear as universal boundary conditions. The values of the parameters would be determined in some still unknown fundamental theory, but in practice the models are described as depending on a few undetermined soft-supersymmetry breaking masses which, when evolved in the well-known effective theory below the unification scale, generate consequences for the masses and couplings of the SUSY particles that can be compared to experiment.

The supersymmetry breaking in such models occurs through a hidden sector at some scale intermediate between the electroweak and Planck scales. For example, there may exist an asymptotically free gauge theory in the hidden sector in which gaugino condensation or some other nonperturbative mechanism occurs at a high scale  $H_{SUSY}$  related by a geometric hierarchy to the Planck and electroweak scales ( $M_{SUSY} \sim H_{SUSY}^n / M_P^{n-1}$ ), thus breaking supersymmetry in the observable sector near the electroweak scale  $M_{SUSY} \sim M_W$ . Since this breaking of supersymmetry occurs in the hidden sector which is coupled only gravitationally to the observable sector, the supersymmetry breaking is suppressed relative to the Planck scale by factors of  $H_{SUSY} / M_P$ . This mechanism gives rise to an effective theory in the observable sector

with softly broken global supersymmetry, giving the scale of the soft-supersymmetry breaking parameters near the electroweak scale. How the effective theory parameters are determined and related to each other depends on the details of the supersymmetry breaking scenario.

## 2 Soft-supersymmetry breaking parameters

Retaining only the dominant Yukawa couplings  $\lambda_t$ ,  $\lambda_b$  and  $\lambda_\tau$ , the superpotential\* is given in terms of the superfields by

$$W = \epsilon_{ij} \left( \lambda_t Q^i H_2^j t^c + \lambda_b Q^i H_1^j b^c + \lambda_\tau L^i H_1^j \tau^c + \mu H_1^i H_2^j \right), \quad (1)$$

where  $Q = (t, b)$ ,  $L = (\tau, \nu_\tau)$  and  $H_1 = (H_1^0, H_1^-)$  and  $H_2 = (H_2^+, H_2^0)$  and  $\epsilon_{ij}$  with  $i, j = 1, 2$  is the antisymmetric tensor in two dimensions. The Yukawa couplings are defined by

$$\lambda_t = \frac{\sqrt{2}m_t}{v \sin \beta}, \quad \lambda_b = \frac{\sqrt{2}m_b}{v \cos \beta}, \quad \lambda_\tau = \frac{\sqrt{2}m_\tau}{v \cos \beta}, \quad (2)$$

where  $\tan \beta = v_2/v_1$  is the ratio of the vacuum expectation values of  $H_2^0$  and  $H_1^0$ . The  $\mu$  term in the superpotential contributes to the Higgs potential which at tree level is

$$V_0 = (m_{H_1}^2 + \mu^2)|H_1|^2 + (m_{H_2}^2 + \mu^2)|H_2|^2 + m_3^2(\epsilon_{ij}H_1^i H_2^j + \text{h.c.}) + \frac{1}{8}(g^2 + g'^2) [ |H_1|^2 - |H_2|^2 ]^2 + \frac{1}{2}g^2 |H_1^{i*} H_2^i|^2, \quad (3)$$

where  $m_{H_1}$ ,  $m_{H_2}$ , and  $m_3$  are soft-supersymmetry breaking parameters. We shall define as usual the soft Higgs mass parameters

$$m_1^2 = m_{H_1}^2 + \mu^2, \quad (4a)$$

---

\*Caution: Our convention for the sign of  $\mu$  (and also the sign of the trilinear couplings  $A$  introduced below) differs from some authors.

$$m_2^2 = m_{H_2}^2 + \mu^2 . \quad (4b)$$

Of the eight degrees of freedom in the two Higgs doublets, three ( $G^\pm, G^0$ ) are absorbed to give the  $W^\pm$  and  $Z$  masses, leaving five physical Higgs bosons: the charged Higgs bosons  $H^\pm$ , the CP-even Higgs bosons  $h$  and  $H$ , and the CP-odd Higgs boson  $A$ .

There are soft-supersymmetry breaking gaugino mass terms

$$\frac{1}{2}M_1\overline{B}B + \frac{1}{2}M_2\overline{W}^aW^a + \frac{1}{2}M_3\overline{\tilde{g}}^b\tilde{g}^b , \quad (5)$$

for the bino  $B$ , the winos  $W^a$  ( $a = 1, 2, 3$ ), and the gluinos  $\tilde{g}^b$  ( $b = 1, \dots, 8$ ).

Corresponding to each superpotential coupling there is a soft-supersymmetry breaking trilinear coupling

$$\epsilon_{ij} \left( \lambda_t A_t \tilde{Q}^i H_2^j \tilde{t}^c + \lambda_b A_b \tilde{Q}^i H_1^j \tilde{b}^c + \lambda_\tau A_\tau \tilde{L}^i H_1^j \tilde{\tau}^c + \mu B H_1^i H_2^j \right) \quad (6)$$

and soft squark and slepton mass terms

$$\begin{aligned} & M_Q^2 [\tilde{t}_L^* \tilde{t}_L + \tilde{b}_L^* \tilde{b}_L] + M_U^2 \tilde{t}_R^* \tilde{t}_R + M_D^2 \tilde{b}_R^* \tilde{b}_R \\ & + M_L^2 [\tilde{\tau}_L^* \tilde{\tau}_L + \tilde{\nu}_L^* \tilde{\nu}_L] + M_E^2 \tilde{\tau}_R^* \tilde{\tau}_R . \end{aligned} \quad (7)$$

The RGE for the soft-supersymmetry breaking parameters are given in the appendix, and the RGE for the gauge and Yukawa couplings are summarized in Ref. [15].

An interesting aspect of the supergravity breaking mechanism is the origin of the  $3-2-1$  supersymmetry at low scales. Why is it the electroweak gauge group the one that is broken, and not QCD? Consider the renormalization group equations from the appendix for the scalar states  $H_2$ ,  $\tilde{t}_R$ , and  $\tilde{Q}_L$  retaining only the QCD gauge coupling

$g_3$  and the top Yukawa coupling  $\lambda_t$  terms[19],

$$8\pi^2 \frac{d}{dt} \begin{pmatrix} M_{H_2}^2 \\ M_{t_R}^2 \\ M_{Q_L}^2 \end{pmatrix} = -\frac{16}{3} g_3^2 M_3^2 \begin{pmatrix} 0 \\ 1 \\ 1 \end{pmatrix} + \lambda_t^2 X_t \begin{pmatrix} 3 \\ 2 \\ 1 \end{pmatrix}, \quad (8)$$

where  $X_t = M_{Q_L}^2 + M_{t_R}^2 + M_{H_2}^2 + A_t^2$  and  $t = \ln Q/M_G$ . The  $\lambda_t^2$  term is the means by which the mass-squares are driven to lower values as the scale decreases. Because the Higgs field is uncolored, the group theory factors allow  $M_{H_2}^2$  to be driven negative with  $M_{t_R}^2$  and  $M_{Q_L}^2$  remaining positive, thus breaking only the electroweak gauge group.

According to conventional wisdom the squarks and sleptons have a universal soft-supersymmetry breaking mass  $m_0$  at the unification scale. Then any deviations from degeneracy at the SUSY scale are suppressed by the associated quark or lepton mass, which is small except for the top squarks. The flavor changing neutral currents (FCNCs) are thereby suppressed to an acceptable level. The universal boundary condition applies in minimal supergravity models with the canonical kinetic energy. Recently there has been some interest in relaxing this condition[20]–[22].

Analytical expressions can be obtained for the squark and slepton mass parameters when the corresponding Yukawa couplings are negligible (i.e. for the first two generations). For a universal scalar mass  $m_0$  and gaugino mass  $m_{\frac{1}{2}}$  at the GUT scale (this condition need not apply in general in string theories), one has the relation

$$m_{\tilde{f}}^2 = m_0^2 + \sum_{i=1}^3 f_i m_{\frac{1}{2}}^2 + (T_{3,\tilde{f}} - e_{\tilde{f}} \sin^2 \theta_w) M_Z^2 \cos 2\beta, \quad (9)$$

for the squark and slepton masses where the  $f_i$  are (positive) constants that depend on the evolution of the gauge couplings

$$f_i = \frac{c_i(f)}{b_i} \left[ 1 - \frac{1}{\left(1 - \frac{\alpha_G}{2\pi} b_i t\right)^2} \right]. \quad (10)$$

Here  $T_{3,\bar{f}}$  is the  $SU(2)$  quantum number and  $e_{\bar{f}}$  is the electromagnetic charge of the sfermion. The  $b_i$  are given in the appendix and  $c_i(f)$  is  $\frac{N^2-1}{N}$  (0) for fundamental (singlet) representations of  $SU(N)$  and  $\frac{3}{10}Y^2$  for  $U(1)_Y$ . The squark mass spectrum of the third generation is more complicated for two reasons: (1) the effects of the third generation Yukawa couplings need not be negligible, and (2) there can be substantial mixing between the left and right top squark fields (and left and right bottom squark fields for large  $\tan\beta$ ) so that they are not the mass eigenstates.

The gaugino evolution is particularly simple by virtue of their simple renormalization group equations; at one-loop order the gaugino masses parameters  $M_1$ ,  $M_2$ , and  $M_3$  scale in exactly the same proportions as do the gauge couplings so that

$$m_{\bar{g}} = M_3(m_t) = \frac{\alpha_3(m_t)}{\alpha_2(m_t)}M_2(m_t) = \frac{\alpha_3(m_t)}{\alpha_1(m_t)}M_1(m_t). \quad (11)$$

Figure 1 shows a typical evolution of the soft-supersymmetry breaking parameters. The characteristic behavior exhibited by the mass parameters are typical of renormalization group equation evolution. The colored particles are generally driven heavier at low  $Q$  by the large strong gauge coupling. The Higgs mass parameter  $m_2^2$  is usually driven negative (at least for  $\tan\beta$  not too small), giving the electroweak symmetry breaking. Assumed universal boundary conditions at the GUT scale yields correlations between the masses in the supersymmetric spectrum.



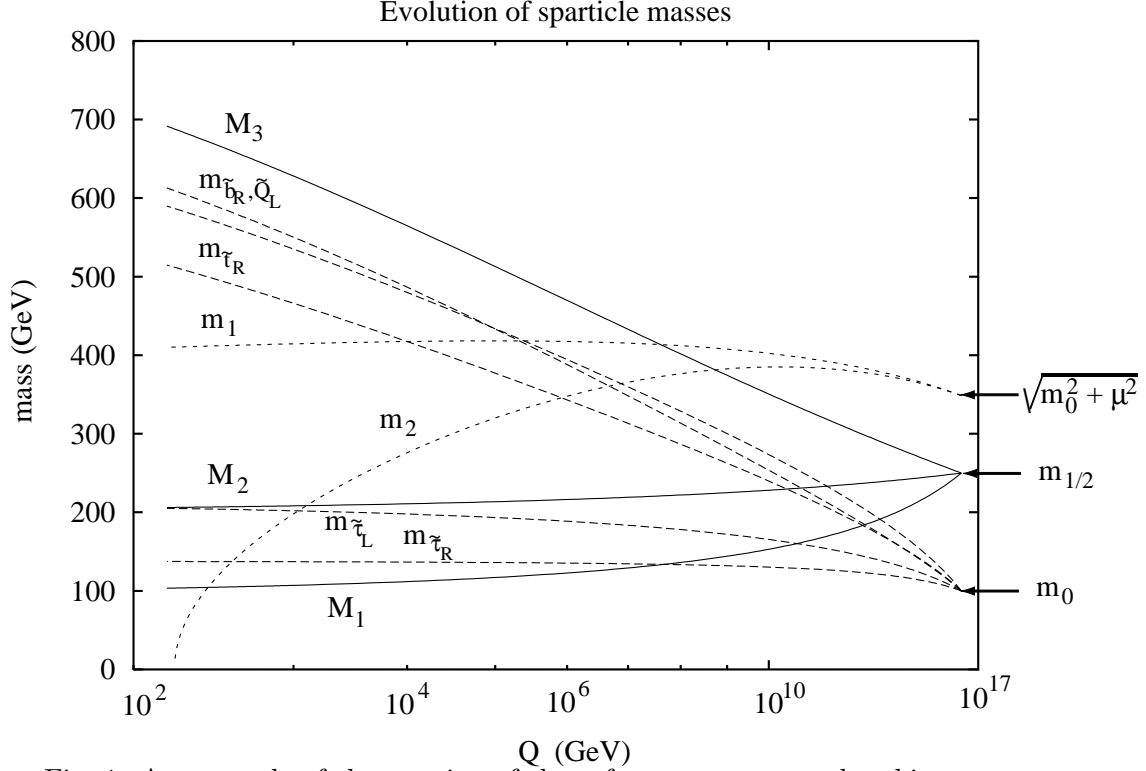


Fig. 1. An example of the running of the soft-supersymmetry breaking parameters for  $\alpha_s(M_Z) = 0.120$ ,  $m_t(m_t) = 150$  GeV,  $\tan\beta = 10$ ,  $m_{\frac{1}{2}} = 250$  GeV,  $m_0 = 100$  GeV, and  $A^G = 0$ , where the superscript  $G$  denotes the GUT scale.

Fixed-point solutions to the RGE predict that the scale of the top-quark mass is naturally large in SUSY-GUT models but depends on  $\tan\beta$ . The prediction is that[15]

$$m_t^{\text{pole}} = (200 \text{ GeV}) \sin\beta. \quad (12)$$

Note that the propagator-pole mass  $m_t^{\text{pole}}$  is related to this running mass  $m_t(m_t)$  by[23]

$$m_t^{\text{pole}} = m_t(m_t) \left[ 1 + \frac{4}{3\pi} \alpha_3(m_t) \right]. \quad (13)$$

### 3 One-Loop Contributions: Tadpole Method

Although the tree level Higgs potential is not reliable for the purpose of analyzing radiative breaking of the electroweak symmetry[6], it provides a convenient starting point for our discussion. Recall the tree level potential Eq. (3). In supergravity models  $m_3^2$  is related to  $B$  and  $\mu$  by

$$m_3^2 = B\mu . \quad (14)$$

When the neutral components of the Higgs doublets receive vacuum expectation values  $v_1$  and  $v_2$ , the potential develops tadpoles. Inserting[24]

$$H_1 = \begin{pmatrix} \frac{1}{\sqrt{2}}(\psi_1 + v_1 + i\phi_1) \\ H_1^- \end{pmatrix} \quad (15a)$$

$$H_2 = \begin{pmatrix} H_2^+ \\ \frac{1}{\sqrt{2}}(\psi_2 + v_2 + i\phi_2) \end{pmatrix} \quad (15b)$$

into Eq. (3) one can identify

$$V_{\text{tadpole}} = t_1\psi_1 + t_2\psi_2 , \quad (16)$$

where  $t_1$  and  $t_2$  are (tree-level) tadpoles:

$$t_1 = (m_{H_1}^2 + \mu^2)v_1 + B\mu v_2 + \frac{1}{8}(g^2 + g'^2)v_1(v_1^2 - v_2^2) , \quad (17a)$$

$$t_2 = (m_{H_2}^2 + \mu^2)v_2 + B\mu v_1 - \frac{1}{8}(g^2 + g'^2)v_2(v_1^2 - v_2^2) . \quad (17b)$$

The minimum of the Higgs potential is determined by setting the first derivatives of the fields to zero,

$$\frac{\partial V_0}{\partial \psi_i} = \frac{\partial V_{\text{tadpole}}}{\partial \psi_i} = 0 . \quad (18)$$

Therefore the tadpoles  $t_1$  and  $t_2$  must vanish at the minimum. With our normalization of  $\psi_1$  and  $\psi_2$  (i.e. including the factor of  $\frac{1}{\sqrt{2}}$  in Eq. (15a) and Eq. (15b)), the  $W$  and  $Z$  masses are

$$M_W^2 = \frac{1}{4}g^2(v_1^2 + v_2^2), \quad (19a)$$

$$M_Z^2 = \frac{1}{4}(g^2 + g'^2)(v_1^2 + v_2^2), \quad (19b)$$

which implies  $v_1^2 + v_2^2 = v^2 = (246\text{GeV})^2$ . A particularly useful form of the minimization conditions is obtained by forming the linear combinations  $T_1$  and  $T_2$  of the tadpoles given by

$$\begin{pmatrix} T_1 \\ T_2 \end{pmatrix} = \begin{pmatrix} \cos \beta & -\sin \beta \\ \sin \beta & \cos \beta \end{pmatrix} \begin{pmatrix} t_1 \\ t_2 \end{pmatrix}. \quad (20)$$

where  $\cos \beta = v_1/v$  and  $\sin \beta = v_2/v$ . From Eqs. (17a) and (17b) we have

$$\begin{aligned} T_1 &= \frac{1}{v} \left[ (m_{H_1}^2 + \mu^2)v_1^2 - (m_{H_2}^2 + \mu^2)v_2^2 + \frac{1}{8}(g^2 + g'^2)v^2(v_1^2 - v_2^2) \right], \\ &= v \left[ (m_{H_1}^2 + \mu^2) \cos^2 \beta - (m_{H_2}^2 + \mu^2) \sin^2 \beta + \frac{1}{8}(g^2 + g'^2)v^2 \cos 2\beta \right], \end{aligned} \quad (21a)$$

$$\begin{aligned} T_2 &= \frac{1}{v} \left[ (m_{H_1}^2 + m_{H_2}^2 + 2\mu^2)v_1v_2 + B\mu v^2 \right], \\ &= v \left[ \frac{1}{2}(m_{H_1}^2 + m_{H_2}^2 + 2\mu^2) \sin 2\beta + B\mu \right]. \end{aligned} \quad (21b)$$

We see that the rotation (20) through the angle  $\beta$  conveniently places all of the dependence on gauge couplings (D-terms) in  $T_1$ . Setting  $T_1 = 0$  and dividing by  $v \cos 2\beta$  yields the familiar tree-level condition

$$\frac{1}{2}M_Z^2 = \frac{m_{H_1}^2 - m_{H_2}^2 \tan^2 \beta}{\tan^2 \beta - 1} - \mu^2. \quad (22)$$

Setting  $T_2 = 0$  and dividing by  $v$  the other tree-level condition

$$-B\mu = \frac{1}{2}(m_{H_1}^2 + m_{H_2}^2 + 2\mu^2) \sin 2\beta, \quad (23)$$

is obtained. Notice that the signs of  $B$  and  $\mu$  are not determined by the minimization conditions (only the relative sign is known), giving rise to two distinct cases.

We can extend the above technique to include one-loop contributions to the Higgs potential, deriving equations analogous to (22) and (23) by setting to zero linear combinations of tadpoles rotated through the angle  $\beta$ . The one-loop effective potential is given by

$$V_1 = V_0 + \Delta V_1, \quad (24)$$

where  $V_0$  is the tree-level Higgs potential and

$$\Delta V_1 = \frac{1}{64\pi^2} \text{Str} \left[ \mathcal{M}^4 \left( \ln \frac{\mathcal{M}^2}{Q^2} - \frac{3}{2} \right) \right], \quad (25)$$

is the one-loop contribution given in the dimensional reduction ( $\overline{DR}$ ) renormalization scheme[25]. The supertrace is defined as  $\text{Str} f(\mathcal{M}^2) = \sum_i C_i (-1)^{2s_i} (2s_i + 1) f(m_i^2)$  where  $C_i$  is the color degrees of freedom and  $s_i$  is the spin of the  $i^{\text{th}}$  particle. To determine the minimum one must set the first derivatives of the effective potential to zero

$$\frac{\partial V_1}{\partial \psi} = \frac{\partial V_0}{\partial \psi} + \frac{1}{32\pi^2} \text{Str} \left[ \frac{\partial \mathcal{M}^2}{\partial \psi} \mathcal{M}^2 \left( \ln \frac{\mathcal{M}^2}{Q^2} - 1 \right) \right] = 0. \quad (26)$$

We note that  $f(m_i^2)$  usually involves the mass eigenstates of the theory; one therefore ought to use the coupling of the Higgs fields to the mass eigenstates in tadpole calculations in order to facilitate comparisons between minimization techniques. Evaluated at the minimum of  $V_1$ , tadpole contributions involve the coupling  $\partial \mathcal{M}^2 / \partial \psi$  and the usual integration factor  $\frac{1}{32\pi^2} \mathcal{M}^2 \left( \ln \frac{\mathcal{M}^2}{Q^2} - 1 \right)$ ; setting tadpole contributions to zero is

therefore equivalent to minimizing the potential. More generally, the  $n$ th derivatives of the effective potential are related to the diagrams (at zero external momentum) with  $n$  external lines; the minimization conditions at one-loop are obtained by calculating diagrams with only one external line – the tadpoles[26, 27].

In order to maintain the linear combinations in (20) for the tree level relations, we calculate with appropriate combinations of Higgs fields in the external Higgs line in the tadpole diagrams. The Feynman rules usually express these external Higgs lines as the physical Higgs bosons  $H$  or  $h$ , which are obtained from the Higgs fields  $\psi_1, \psi_2$  by a rotation by an angle  $\alpha$  (in the opposite direction to the rotation  $\beta$  performed above)

$$\begin{pmatrix} H \\ h \end{pmatrix} = \begin{pmatrix} \cos \alpha & \sin \alpha \\ -\sin \alpha & \cos \alpha \end{pmatrix} \begin{pmatrix} \psi_1 \\ \psi_2 \end{pmatrix}. \quad (27)$$

As with the tree-level tadpoles, we need to rotate the one-loop contributions by the same angle  $\beta$  in order to express the minimization conditions most simply. We therefore define the desired linear combinations  $\mathcal{J}, \mathcal{J}_\perp$  of Higgs fields

$$\begin{pmatrix} \mathcal{J} \\ \mathcal{J}_\perp \end{pmatrix} = \begin{pmatrix} \cos \beta & -\sin \beta \\ \sin \beta & \cos \beta \end{pmatrix} \begin{pmatrix} \psi_1 \\ \psi_2 \end{pmatrix} = \begin{pmatrix} \cos(\beta + \alpha) & -\sin(\beta + \alpha) \\ \sin(\beta + \alpha) & \cos(\beta + \alpha) \end{pmatrix} \begin{pmatrix} H \\ h \end{pmatrix}. \quad (28)$$

To include the one-loop corrections, we calculate the tadpole diagrams in Figure 2, and add the suitably regularized result to the tree-level results.

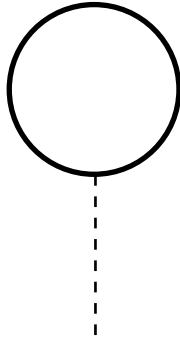


Fig. 2. The one-loop tadpole diagram. The loop consists of matter and gauge-Higgs contributions.

This tadpole technique is not new, and is equivalent to procedures followed previously. However it provides an alternate way of organizing the calculation and of understanding why the contributions have their particular form. Moreover, the analytical expressions obtained with the tadpole technique are often very useful, particularly in certain regions of parameter space that are difficult to explore by simply minimizing the potential numerically (e.g. the low- $\tan\beta$  fixed-point region).

The method of determining the minimization conditions at one-loop by calculating tadpoles is especially convenient for including the corrections from the gauge and Higgs sectors. The loop integrals are standard, and the only work is to determine the coupling between the particle in the loop and the Higgs bosons  $\mathcal{J}$  and  $\mathcal{J}_\perp$  in Eq. (28). This approach is easier than including the field dependent masses in the formal expression in Eq. (25) and then numerically finding the potential minimum. On the other hand, calculating tadpoles alone determines only the first derivatives of the one-loop Higgs potential, and does not yield by itself the Higgs potential away from the minimum. Fortunately, the minimization conditions are all one needs for many analyses.

It is crucial to include the one-loop corrections in the effective potential in determining the vevs. As shown by Gamberini, Ridolfi, and Zwirner[6], the tree-level Higgs vevs  $v_1$  and  $v_2$  are very sensitive to the scale at which the renormalization group equations are evaluated. Thus it is necessary to determine the proper scale at which there are no large logarithms so that the tree-level results are reliable. As is well known, there is a simple hierarchy of scales in these theories. As the soft-supersymmetry breaking parameters are evolved down from the high scale, the Higgs potential evolves so that an asymmetric minimum develops at some scale  $\mu_0$ . This scale is determined by the condition

$$m_1^2(\mu_0)m_2^2(\mu_0) - B^2\mu^2(\mu_0) = 0. \quad (29)$$

For  $Q > \mu_0$ , the vevs  $v_1$  and  $v_2$  vanish. For  $Q < \mu_0$  the vevs become nonzero. In the supergravity theories under consideration  $m_{H_2}^2$  becomes negative, allowing Eq. (29) to be satisfied. Figure 3 describes the potential in the regions of interest[28].

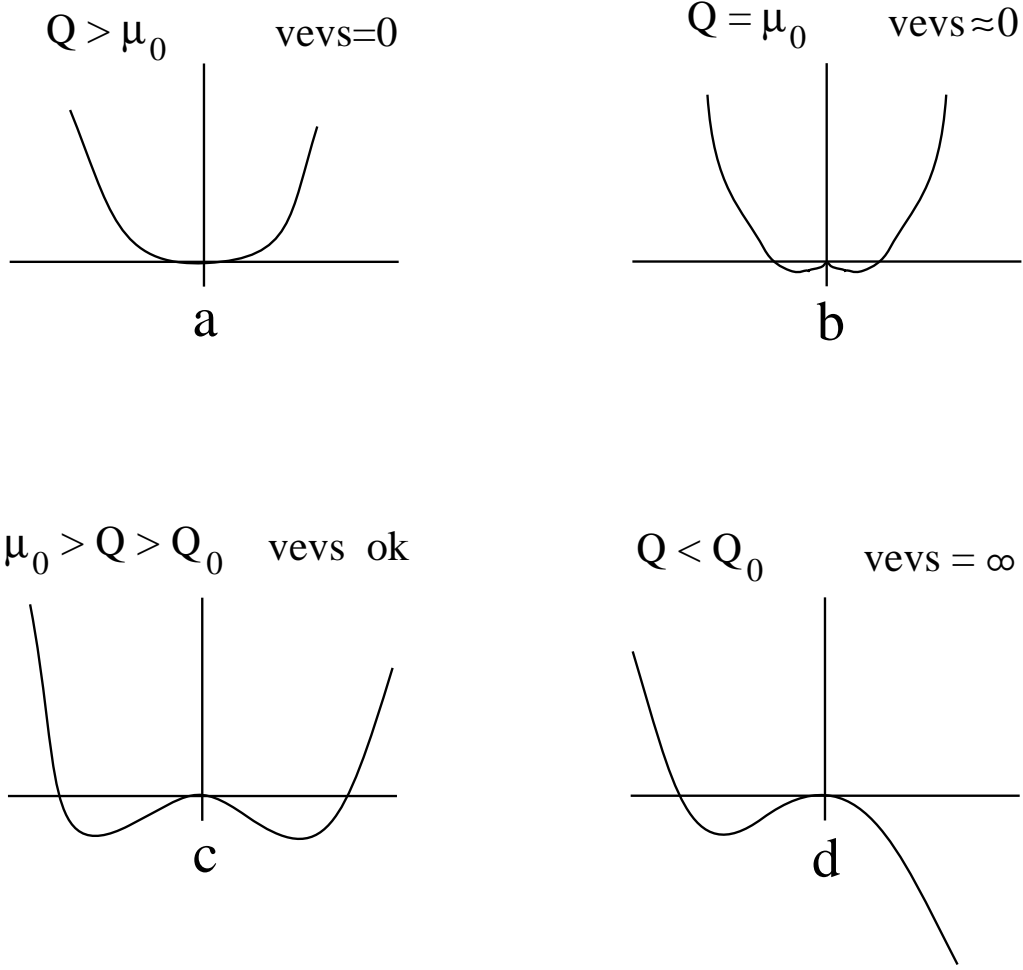


Fig. 3. (a) The vevs vanish for  $Q > \mu_0$ . (b) For  $Q \approx \mu_0$ , the vevs become nonvanishing but small. (c) For some scale  $Q$  in the range  $Q_0 < Q < \mu_0$  the vevs have the correct magnitudes to give correct electroweak symmetry breaking. (d) For  $Q < Q_0$  the potential becomes unbounded from below.

At some lower scale  $Q_0 < \mu_0$ , the Higgs potential becomes unbounded from below.

The scale  $Q_0$  at which this occurs is determined by the condition

$$m_1^2(Q_0) + m_2^2(Q_0) - 2|B(Q_0)\mu(Q_0)| = 0. \quad (30)$$

This implies that in the tree-level potential the vevs  $v_1$  and  $v_2$  must be driven off to infinity because the potential becomes unbounded from below. Because the vevs evolve from zero at or above the scale  $\mu_0$  all the way to infinity at the scale  $Q_0$ , the



vevs are very sensitive to the scale at which they are evaluated.

The solution to this conundrum was provided in Ref. [6]. The inclusion of the one-loop contributions to the Higgs potential stabilizes the vevs with respect to the scale  $Q$  at which the parameters (which evolve according to renormalization group equations) are evaluated. The standard three cases considered are (i)  $M_{\text{SUSY}} < Q_0 < \mu_0$ , (ii)  $Q_0 < M_{\text{SUSY}} < \mu_0$ , and (iii)  $Q_0 < \mu_0 < M_{\text{SUSY}}$ . In case (i) the scale  $Q_0$  is determined by dimensional transmutation in the sense of Coleman and Weinberg[29]. It was initially realized that the one-loop contributions were important in this case, because the minimum of the Higgs potential is driven to the flat direction (“D-flat”) at  $\tan \beta = 1$ [30], and it was crucial to include the one-loop contribution to lift this degeneracy. This yields a light Higgs boson at tree-level (exactly zero mass if  $\tan \beta = 1$ ), which is still acceptable experimentally when the one-loop corrections to the Higgs boson mass are included[24]. However the predicted SUSY mass spectrum is light and already experimentally excluded. Case (ii) has been the subject of much recent work. Case (iii) is not of interest since electroweak symmetry breaking does not occur.

To determine the minimum of the potential, we include the one-loop tadpole contributions

$$T_1 + \Delta T_1 = 0, \tag{31a}$$

$$T_2 + \Delta T_2 = 0. \tag{31b}$$

The contributions  $\Delta T_1$  and  $\Delta T_2$  are given in the Appendix.

## 4 Absence of fine-tuning

The requirement that the supergravity model not be fine-tuned has been recently applied to limit the region of parameter space. This constraint requires that the scale of supersymmetry breaking not be too high. Obtaining reasonable criteria for declaring a particular theory unnaturally fine-tuned remains a subject of debate.

The fine-tuning constraint becomes particularly restrictive in the small and large  $\tan\beta$  regions. For small  $\tan\beta$  (near one), the Higgs potential has its minimum near the D-flat direction. This implies naturally large vevs. Then there must be a cancellation between the two large terms on the right hand side of Eq. (22) to obtain the experimentally observed value for  $M_Z$ . Hence for  $\tan\beta \rightarrow 1$ , the supersymmetric Higgs mass parameter  $\mu$  must be tuned ever more precisely – the fine-tuning problem. In this section we discuss the various attempts to quantify this constraint.

The kinds of criteria advocated by other authors are as follows

- Barbieri and Giudice[31] introduced a naturalness criteria

$$\left| \frac{a_i}{M_Z^2} \frac{\partial M_Z^2}{\partial a_i} \right| < \Delta \quad , \quad (32)$$

for various fundamental parameters  $a_i = m_0, m_{\frac{1}{2}}, \mu^G, A^G, B^G$  to obtain an upper bound on the supersymmetric particle masses. They required that  $\Delta < 10$ , i.e. no cancellations greater than an order of magnitude.

- Lopez, et al.[9] define several fine-tuning coefficients e.g.

$$\frac{\delta M_Z}{M_Z} = c_\mu \frac{\delta \mu}{\mu} . \quad (33)$$

They show that a reasonable upper bound on the simplest coefficient  $c_\mu$  implies an upper bound on  $\mu$ .

- Arnowitt and Nath[7] require that  $m_0 < 1$  TeV, a condition that is easily applied phenomenologically.
- Ross-Roberts[8] and de Carlos and Casas[32] consider the fine-tuning of  $M_Z$  in terms of  $\lambda_t$

$$\frac{\delta M_Z^2}{M_Z^2} = c \frac{\delta \lambda_t^2}{\lambda_t^2}, \quad (34)$$

where  $c$  is required to be less than some small number e.g.  $c \lesssim 10$ . Ross and Roberts who work strictly with the tree-level Higgs potential argue that  $\tan \beta \gtrsim 2$ , while de Carlos and Casas argue that the one-loop corrections to the Higgs potential ameliorate the fine-tuning.

- Olechowski and Pokorski[10] look at a full set of derivatives as in Eq. (33), (34)

$$\frac{\delta Q_j}{Q_j} = \Delta_{ij} \frac{\delta P_i}{P_i}, \quad (35)$$

where the  $Q_j$  are the electroweak scale parameters  $\lambda_t$ ,  $\lambda_\tau$ ,  $v$ ,  $\tan \beta$ ,  $M_A$ ,  $M_Q$ ,  $M_U$ , and the  $P_i$  are the GUT scale parameters  $\lambda_t^G$ ,  $\lambda_\tau^G$ ,  $m_{\frac{1}{2}}$ ,  $m_0$ ,  $\mu^G$ ,  $A^G$ ,  $B^G$ . They also find that small  $\tan \beta$  tends to be more unnatural, and moreover for large values of  $\tan \beta$ , near where the top and bottom quark couplings are equal, that the model becomes rapidly more fine-tuned as  $\tan \beta$  is increased. These constraints are clearly quite involved. While they test a panoply of fine-tuning relations, we feel they are overly complex for such a qualitative and arbitrary

notion as naturalness. Therefore we abandon this notion in favor of a more intuitive definition similar to Lopez. et al.[9].

- Castaño, Piard, and Ramond[11] choose a numerical definition in which the number of iterations the computer has to find a solution is limited. It is not obvious how this algorithm compares quantitatively to those defined above.

Our physical definition of naturalness is simply  $|\mu(M_Z)| \simeq |\mu(m_t)| < 500$  GeV. A measure of the reasonableness of this definition is the effect that small changes in  $\mu$  have on  $M_Z$ . From the tree level equation for  $M_Z$  (see Eqn. (22)) it is readily apparent that larger values of  $|\mu|$  become more unnatural. In Figure 4 we plot the dependence of  $M_Z$  on  $\mu$  and  $B$  for both the tree-level calculation and the full one-loop contributions to the Higgs potential. It can be seen that the one-loop contributions reduce the fine-tuning to an extent. This comparison can be related to the plots of the vevs as a function of scale  $Q$  as discussed in Ref. [32].

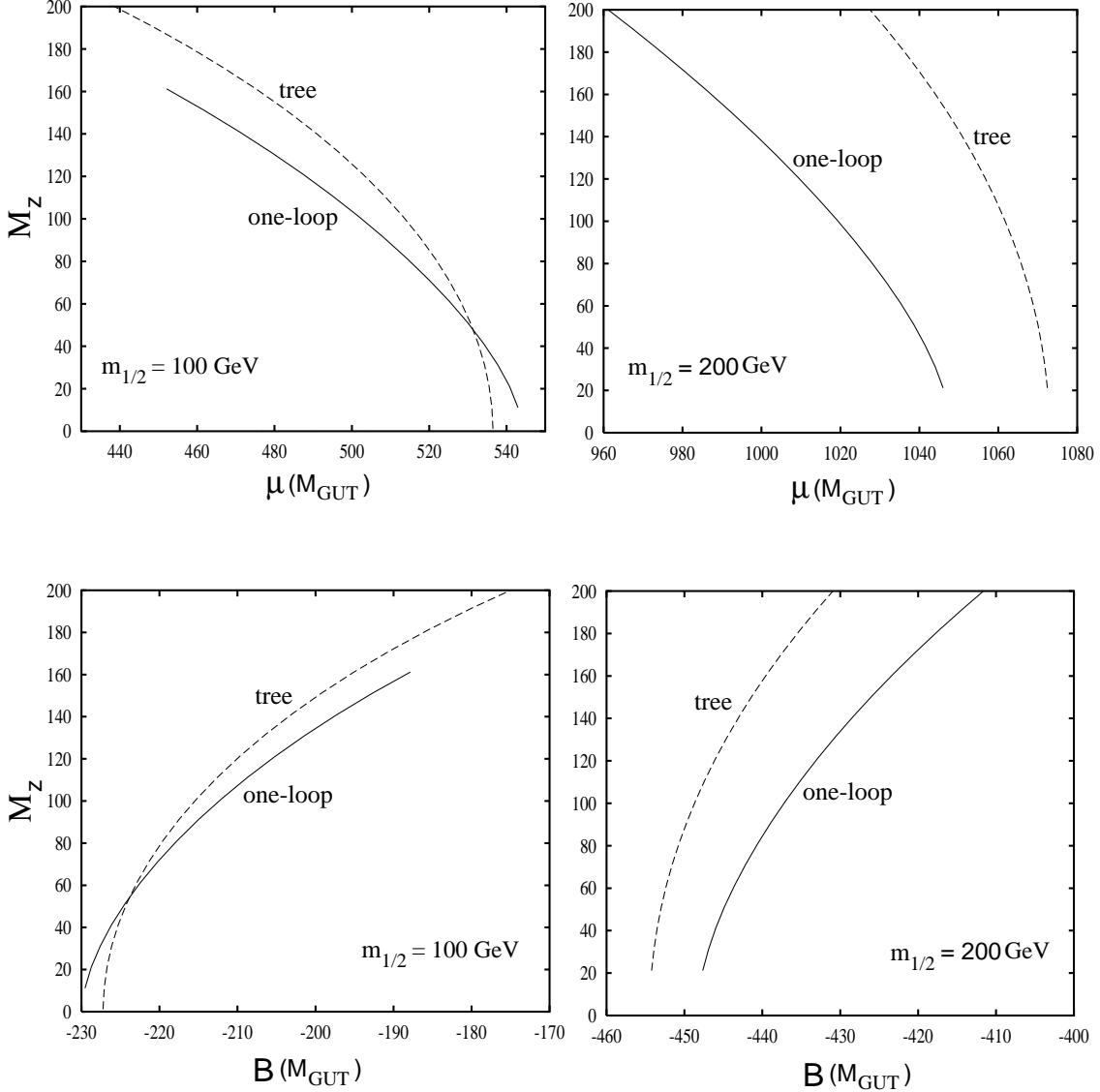


Fig. 4. The change in  $M_Z$  with  $\mu$  and  $B$  for the fixed-point solution  $m_t(m_t) = 160$ ,  $\tan \beta = 1.47$ ,  $m_0 = 0$ ,  $A^G = 0$ , and two different values of  $m_{\frac{1}{2}}$ . The values of  $\mu(M_G)$  meet our naturalness criterion  $|\mu(M_Z)| < 500$  GeV. The solid (dashed) curves are the results at one-loop (tree) level. The case  $\mu < 0$  gives comparable curves.

The plots in Figure 4 correspond to a low- $\tan \beta$  fixed-point solution[15]–[18]; in such cases the tree-level and one-loop-level values turn out to be comparable for either  $\mu$  and  $B$  in the region defined by our naturalness criterion (only the degree of fine-tuning changes). Consequently, including the one-loop corrections in the Higgs

potential does not have a critical impact on the phenomenology. This result does not extend to other regions of the  $m_t$ - $\tan\beta$  plane since there our criterion for naturalness implies a larger allowed range of  $m_0$  and  $m_{\frac{1}{2}}$  in which the one-loop contributions can change  $\mu$  and  $B$  significantly (see section 7).

One can consider quantitative fine-tuning criteria analogous to those considered above,

$$\begin{aligned}\frac{\delta M_Z}{M_Z} &= c_\mu \frac{\delta\mu^G}{\mu^G}, \\ \frac{\delta M_Z}{M_Z} &= c_B \frac{\delta B^G}{B^G},\end{aligned}\tag{36}$$

with e.g.  $|c_\mu|, |c_B| \lesssim 30$ , where the derivatives on the left hand side are obtained at the physical  $Z$  mass scale and the derivatives on the right hand side are at the GUT scale (denoted by the  $G$  superscript). Since the RGE equation for  $\mu$  is proportional to  $\mu$ , the value of  $\delta\mu/\mu$  is scale independent, but  $\delta B/B$  depends on scale. Table 1 gives the values of  $|c_\mu|$  and  $|c_B|$  determined for the tree-level and one-loop curves for the low- $\tan\beta$  fixed point solution of Figure 4.

$m_{\frac{1}{2}}$	$ c_\mu , (\mu > 0)$	$ c_B , (\mu > 0)$	$ c_\mu , (\mu < 0)$	$ c_B , (\mu < 0)$
100 GeV (loop)	8.8	8.2	7.3	5.2
100 GeV (tree)	13.5	10.9	13.5	6.3
200 GeV (loop)	25.6	27.0	20.3	16.9
200 GeV (tree)	57.0	46.8	57.0	27.6

**Table 1:** Values of  $|c_\mu|$  and  $|c_B|$  obtained at tree and one-loop levels for the fixed-point solution of Figure 5.

Note that inclusion of the full one-loop contribution substantially reduces the fine-tuning constants  $|c_\mu|$  and  $|c_B|$ . Our entries for  $|c_\mu|$  are somewhat larger than those found in Ref. [9] because our model has a value of  $\tan\beta$  that is closer to  $\tan\beta = 1$ .

## 5 Models

The introduction of supersymmetry introduces many new unknown parameters to the standard model. The advantage of the popular supergravity models is that this number of new parameters is reduced to five or less. The models discussed here should only be viewed as examples of possible supersymmetry breaking scenarios. Some features may be more general, however.

### A. General model[5]

The universal parameters at the GUT scale are  $m_0$ ,  $A^G$ ,  $m_{\frac{1}{2}}$ ,  $\mu^G$ ,  $B^G$ . In the minimal supergravity model, these five parameters describe the higgsino and gaugino sectors. The universality of the scalar masses at the GUT scale provides for the suppression of dangerous flavor changing neutral currents involving the squarks of the first two generations.

### B. No-scale[30, 33]

In no-scale models two of the five parameters are zero at the unification scale,

$$m_0 = 0, \quad A^G = 0. \quad (37)$$

Thus the scalar fields are massless there, and  $m_{\frac{1}{2}}$  is the sole origin of supersymmetry breaking.

### C. Strict no-scale[30, 33]

The strict no-scale model is a version of the no-scale model with

$$B^G = 0, \tag{38}$$

at the unification scale.

**D. Dilaton[20]**

When the dilaton  $S$  receives a vev, one encounters a breaking of supersymmetry that is of a different nature than that of the minimal supergravity scenarios described above. The dilaton F-term scenario leads to simple boundary conditions for the soft-supersymmetry parameters

$$m_0 = \frac{1}{\sqrt{3}}m_{\frac{1}{2}}, \quad A^G = -m_{\frac{1}{2}}. \tag{39}$$

This model therefore has only three parameters. When it is required that  $\mu$  receive contributions from supergravity only, the additional unification constraint

$$B^G = 2m_0, \tag{40}$$

is obtained. The dilaton version of supersymmetry breaking has been studied in the MSSM in Ref. [34] and for the flipped SU(5) model in Ref. [35].

**E. String-Inspired**

Supersymmetry breaking in strings is a nonperturbative effect, since supersymmetry is preserved order by order in perturbation theory. Very little is known about nonperturbative effects in string theory. Recently the authors of Ref. [21] have proposed to parametrize our ignorance of the exact nature of the breakdown of supersymmetry. The dilaton breaking scenario above is a specific case of more general



scenario of supersymmetry breaking in which the moduli fields  $T_m$  also receive a vev. If one restricts oneself to the case where only one  $T$  field and the dilaton  $S$  get vevs, then the amount of SUSY breaking that arises from each sector can be parametrized by the “goldstino angle[21]”  $\theta$ . The dilaton breaking case corresponds to  $\sin \theta = 1$ . The angle  $\theta$  is constrained by low-energy phenomenology since purely dilaton breaking gives a universal boundary condition for the scalar masses, and the breaking of supersymmetry when the moduli field gets a vev will give rise to FCNCs in the low-energy theory. According to Ref. [21] the more general case, where substantial contributions to supersymmetry breaking arise from the moduli field getting a vev, is not ruled out.

The unification scale in the string-inspired model is roughly an order of magnitude higher than the scale at which the gauge couplings unify in the MSSM. Presumably large threshold corrections due to non-degenerate GUT particles could account for this discrepancy.

### **F. Large $\tan \beta$ scenario[36]**

The correct electroweak symmetry breaking does not occur for too large values of  $\tan \beta$ . If  $\tan \beta \gtrsim m_t(m_t)/m_b(m_t)$ , then the bottom quark Yukawa drives the Higgs masses parameter  $m_1^2$  negative first (instead of  $m_2^2$  from the top quark Yukawa coupling). For  $\tan \beta$  close to this limit considerable fine-tuning is required to get the correct electroweak scale. This situation is ameliorated somewhat with the inclusion of the one-loop corrections in the effective potential[10].

## 6 Ambidextrous Approach to RGE Integration

Previous RGE studies of the supersymmetric particle spectrum have evolved from inputs at the GUT scale (the top-down method[9, 11]) or from inputs at the electroweak scale (the bottom-up approach[10]). Our approach incorporates some boundary conditions at both electroweak and GUT scales, which we call the ambidextrous approach. We specify  $m_t$  and  $\tan\beta$  at the electroweak scale (along with  $M_Z$  and  $M_W$ ) and  $m_{\frac{1}{2}}$ ,  $m_0$ , and  $A^G$  at the GUT scale. The soft supersymmetry breaking parameters are evolved from the GUT scale to the electroweak scale and then  $\mu(M_Z)$  and  $B(M_Z)$  (or  $\mu(m_t)$  and  $B(m_t)$ ) are determined by the tadpole equations at one-loop order. Subsequently  $\mu$  and  $B$  can be RGE-evolved up to the GUT scale. This strategy is effective because the RGEs for the soft-supersymmetry breaking parameters (see the appendix) do not depend on  $\mu$  and  $B$ . This method has two powerful advantages: First, any point in the  $m_t - \tan\beta$  plane can be readily investigated in specific supergravity models since  $m_t$  and  $\tan\beta$  are taken as inputs. Second, the tadpole equations Eq. (79a-79b) are easy to solve in the ambidextrous approach. The  $T_1$  equation can be solved iteratively for  $\mu(M_Z)$ , and then the  $T_2$  equation explicitly gives  $B(M_Z)$ . We stress the numerical simplicity: no derivatives need be calculated and no functions need to be numerically minimized.

We now describe our numerical approach in more detail. Starting with our low-energy choices for  $m_t$ ,  $\tan\beta$ ,  $\alpha_3$ , and  $m_b$  (and using the experimentally determined values for  $\alpha_1$ ,  $\alpha_2$  and  $m_\tau$ [37]), we integrate the MSSM RGEs from  $m_t$  to  $M_G$  with  $M_G$  taken to be the scale  $Q$  at which  $\alpha_1(Q) = \alpha_2(Q)$ . We then specify  $m_{\frac{1}{2}}$ ,  $m_0$ , and

$A^G$ , and integrate back down to  $m_t$  where we solve the tadpole equations for  $\mu(m_t)$  and  $B(m_t)$ . We can then integrate the RGEs back to  $M_G$  to obtain  $\mu^G$  and  $B^G$  at  $M_G$ . A few remarks are pertinent:

1) We integrate the two-loop MSSM RGEs for the gauge and Yukawa couplings[15], but only the one-loop MSSM RGEs (as given in the appendix) for the other supersymmetric parameters. We retain the important two-loop gauge and Yukawa effects (only the two-loop gaugino RGEs exist[38] and we desire to be consistent with regard to the order for the soft-supersymmetry breaking parameters).

2) Since we are working only to one-loop order in most RGEs, we neglect threshold effects at both the GUT[39]–[42] and supersymmetry scales. To properly take into account threshold effects requires that the appropriate beta functions be calculated at every (s)particle threshold, and since the complete supersymmetric mass spectrum and the GUT particle spectra are generally not known a priori, the calculation and use of these beta functions is extremely daunting. In any event, it should not be critical to incorporate these threshold effects into a one-loop calculation since two-loop contributions will be comparable to threshold effects.

3) We take the lower bound of our integration at  $m_t$  instead of  $M_Z$  for several reasons. As shown by several groups[6, 9, 10, 11, 32], inclusion of the one-loop effects into the effective potential makes electroweak symmetry breaking roughly independent of scale; the scale  $Q = m_t$  is roughly the value for which the large logs cancel among themselves in the one-loop corrections to the minimization conditions. We choose  $m_t$  as the boundary since the RGEs (in particular for the gauge and Yukawa

couplings) are simple at scales above  $m_t$ , and it is non-trivial to extend them below  $m_t$ . In addition, the choice of  $m_t$  facilitates comparison with previous work on gauge and Yukawa unification and fixed points.

## 7 Results

We discuss the supersymmetric spectrum and phenomenology for several representative points in the  $m_t - \tan\beta$  plane. For the most part we focus on the low- $\tan\beta$  fixed-point region since it is very attractive to explain the large top quark mass as a fixed point phenomenon[15]–[18]. Moreover, the supersymmetric spectrum in this region is largely unexplored, probably due to fears of excessive fine-tuning. However, as addressed in Section 4, these fears are not necessarily justified; there remains substantial viable parameter space for which fine-tuning does not pose great concern, particularly with the inclusion of the full one-loop corrections to the effective potential[10].

The  $m_t - \tan\beta$  parameter space can be divided into several distinct regions, as shown in Figure 5.

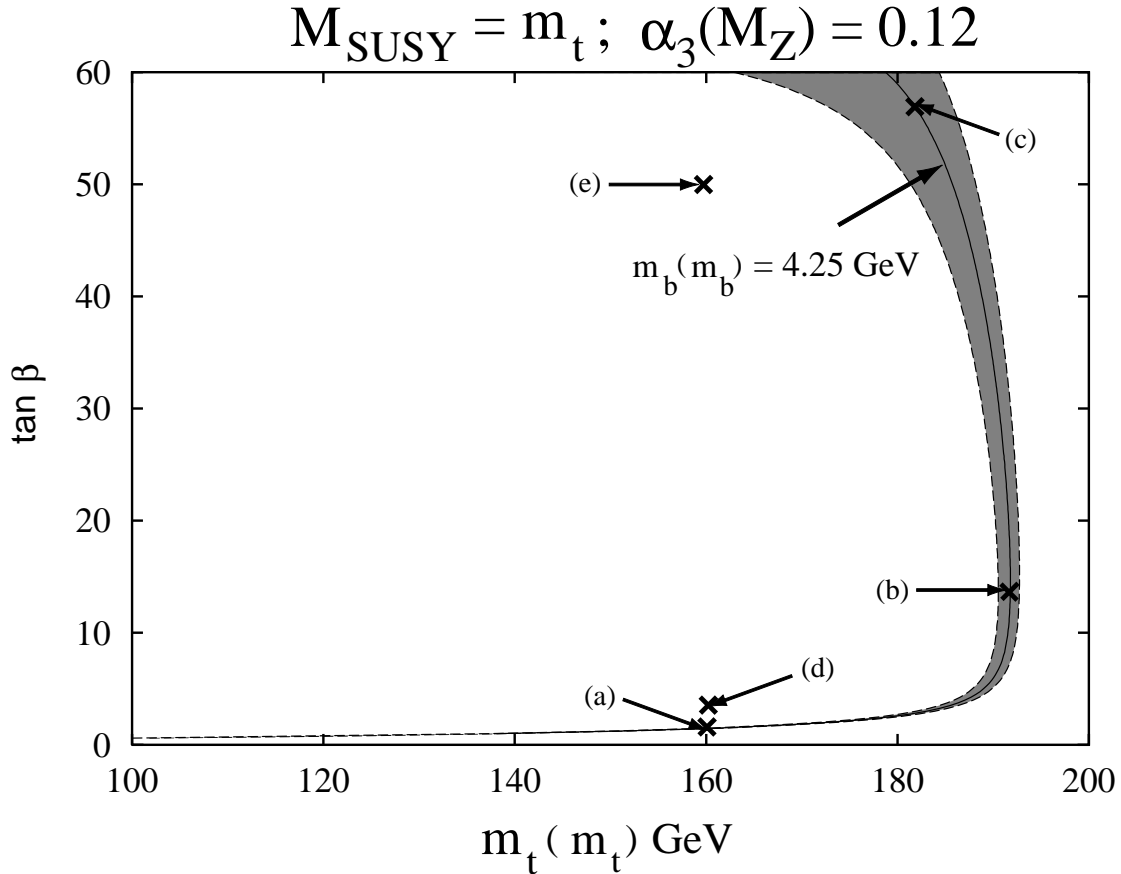


Fig. 5. The allowed  $m_t - \tan\beta$  parameter space assuming Yukawa unification  $\lambda_b(M_G) = \lambda_\tau(M_G)$ . [15]. The shaded area indicates the region for which  $m_b(m_b) = 4.25 \pm 0.15$  GeV. Points representative of distinct regions within this parameter space are denoted with labels (a)-(e).

We discuss the supersymmetric mass spectrum for each of these regions. Unless otherwise specified, we take  $A^G = 0$ ,  $\alpha_3(M_Z) = 0.120$ , and  $m_b(m_b) = 4.25$  GeV. The qualitative behaviour in each region should not depend greatly on these parameters.

- **(a) Low- $\tan\beta$  Fixed Point**

As a typical example of the low  $\tan\beta$  fixed values region we consider the point  $m_t(m_t) = 160$  GeV,  $\tan\beta = 1.47$  (for which  $\lambda_t(M_G) = 2.7$ ). We aim to determine the GUT-scale parameter space for which this solution can be obtained

from the minimization of the effective potential. Using the tadpole method, we explore a grid of  $m_0$  and  $m_{\frac{1}{2}}$  values and apply both experimental and naturalness bounds. For the lower experimental limits, we adopt the values listed in Table 2 following Ref. [43].

Particle	Experimental Limit (GeV)
gluino	120
squark, slepton	45
chargino	45
neutralino	20
light higgs	60

**Table 2:** Approximate experimental bounds that we apply in Figure 6.

Figure 6 shows the allowed parameter space for both signs of  $\mu$  along with the most restrictive constraints in each case. The contours of constant  $|\mu|$  are ellipses in the  $m_0 - m_{\frac{1}{2}}$  plane for  $|\mu| \gg M_Z$ .

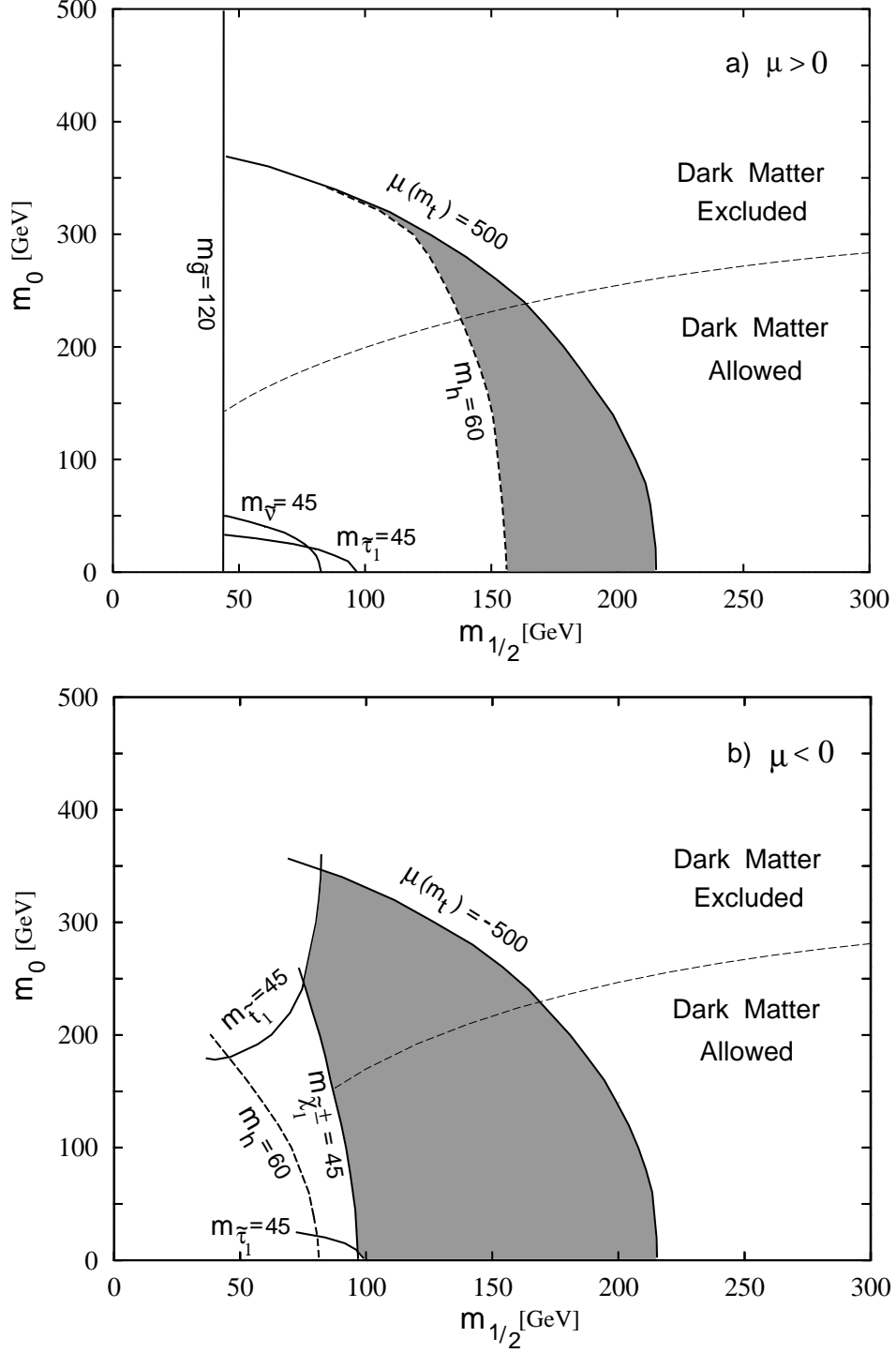


Fig. 6. The allowed  $m_0, m_{\frac{1}{2}}$  region is shaded for the low-tan  $\beta$  fixed point  $m_t(m_t) = 160$  GeV,  $\tan \beta = 1.47$  solution with (a)  $\mu > 0$  and (b)  $\mu < 0$ . The experimental bounds in Table 2 and the naturalness bound  $|\mu(m_t)| < 500$  GeV are imposed with  $A^G = 0$  GeV. A semi-quantitative dark matter constraint (given by Eq. (45)) is also shown.

Note that the  $\mu < 0$  case has more available parameter space; it is also slightly more *natural*, as indicated from the fine-tuning constants given in Table 1.

We have indicated the light scalar higgs experimental limit with a dashed line in Figure 6; care must be taken when enforcing this particular constraint since the allowed parameter space is somewhat sensitive to the exact  $m_h$  limit. Moreover, the  $m_h$  bound includes only the one-loop quark-squark contributions given in reference[44], and it is expected that inclusion of the chargino and neutralino contributions can affect the mass of the light scalar higgs by a few GeV[45]. In general an increase in  $m_h$  (as in all the experimental constraints) tends to increasingly restrict the allowed parameter space, while a decrease in  $m_h$  has the opposite effect.

Overall we find substantial phenomenologically viable parameter space, especially for  $\mu < 0$ . However the maximal values of the GUT parameters  $m_0$  and  $m_{\frac{1}{2}}$  are not large ( $m_0 \lesssim 350$  GeV,  $m_{\frac{1}{2}} \lesssim 225$  GeV) implying a rather light low energy supersymmetric mass spectrum. Also included in Figure 6 is the semi-quantitative dark matter constraint of Drees and Nojiri [46] (see Eq. (45) below). For this low  $\tan\beta$  fixed-point case it implies that  $m_0 \lesssim 250$  GeV, though this approximate bound ought not to be taken strictly.

We now investigate the supersymmetric particle mass spectra dependence on  $m_0$  and  $m_{\frac{1}{2}}$  independently for this low  $\tan\beta$  fixed-point solution. Figure 7 shows the dependence of the supersymmetric spectrum on  $m_{\frac{1}{2}}$  in the noscale model ( $m_0 = 0$ ). For the squarks and sleptons we plot the light-



est mass eigenstates; in addition we plot the heaviest stop,  $m_{\tilde{t}_2}$ , for reference. We label the chargino and neutralino masses such that  $M_{\chi_1^\pm} < M_{\chi_2^\pm}$  and  $M_{\chi_1^0} < M_{\chi_2^0} < M_{\chi_3^0} < M_{\chi_4^0}$ .

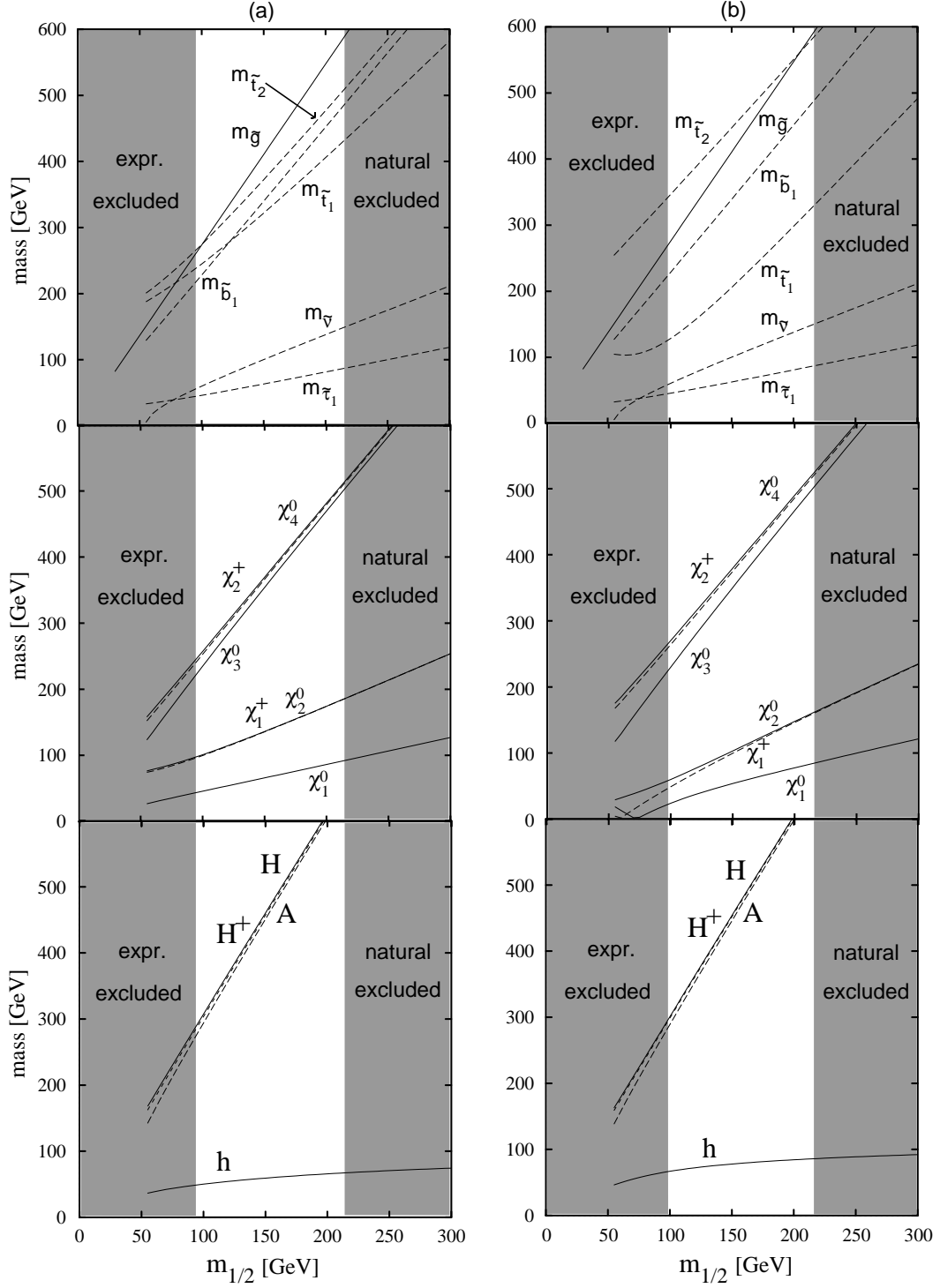


Fig. 7. The low  $\tan\beta$  fixed point solutions for (a)  $\mu > 0$  and (b)  $\mu < 0$  with  $m_0 = 0$  GeV and  $A^G = 0$ . The experimentally excluded region includes all experimental constraints except for the bound on  $m_h$ , since it is sensitive to chargino and neutralino contributions[45].

Figure 8 shows all the squark and slepton masses for the same low- $\tan\beta$  fixed-point solution with  $\mu > 0$ . Note that the squarks of the first two generations can be heavier than those of the third; the up and charm squarks are degenerate as are the down and strange squarks. The slepton masses are approximately generation independent in this case, though this need not be true in general (e.g. see Table 3 below).

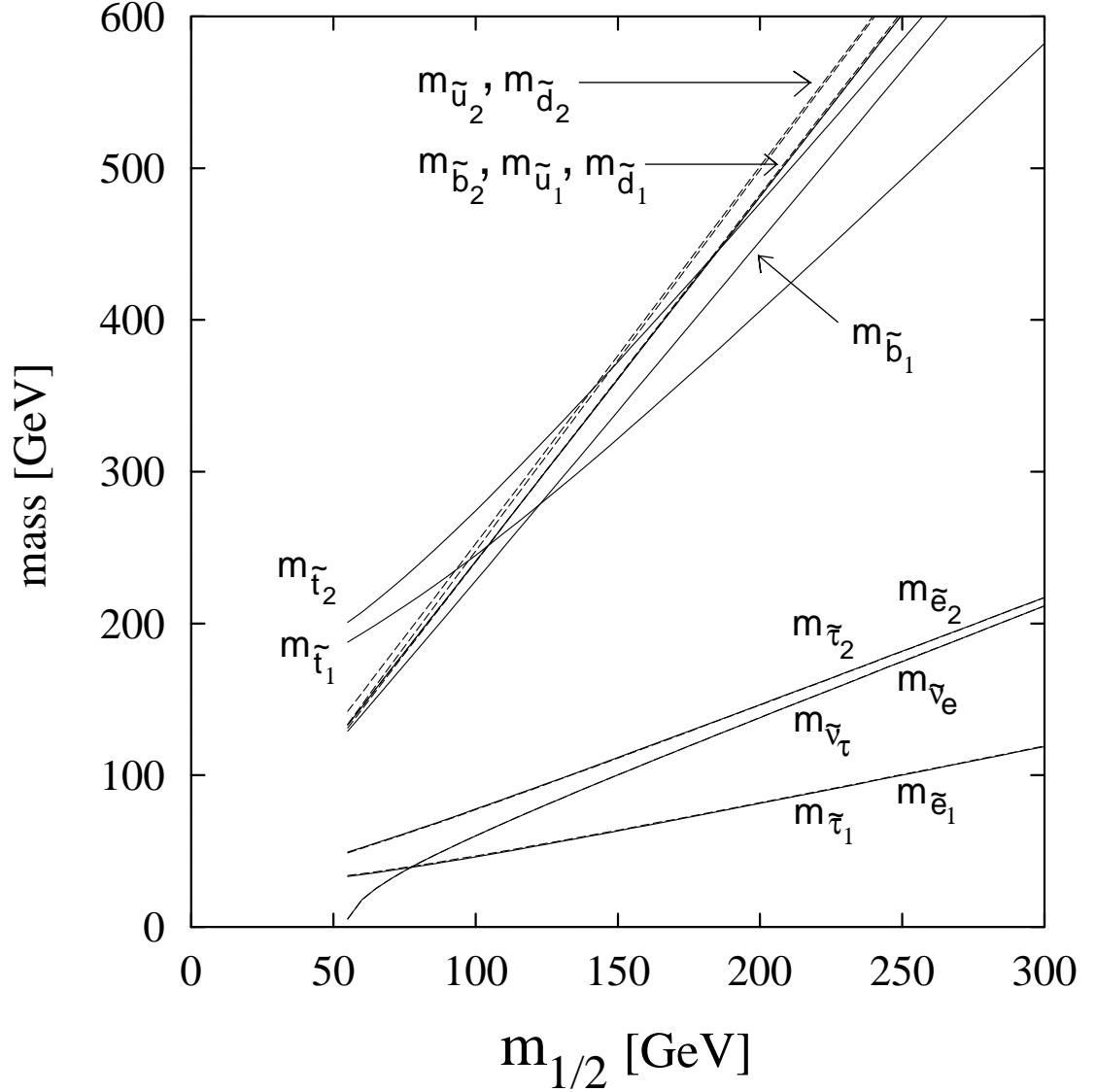


Fig. 8. The squark and slepton masses for the low- $\tan\beta$  fixed-point solution in the no-scale model with  $\mu > 0$ . The solid (dashed) lines correspond to the third (first and second) generation. The excluded regions are the same as in the previous figure.

Figure 9 illustrates the dependence of the supersymmetric spectrum on  $m_0$ . (Here we take  $m_{\frac{1}{2}} = 150$  GeV.) The mass of most of the SUSY particles increase with increasing  $m_0$  (see, e.g. Eq. (9)).

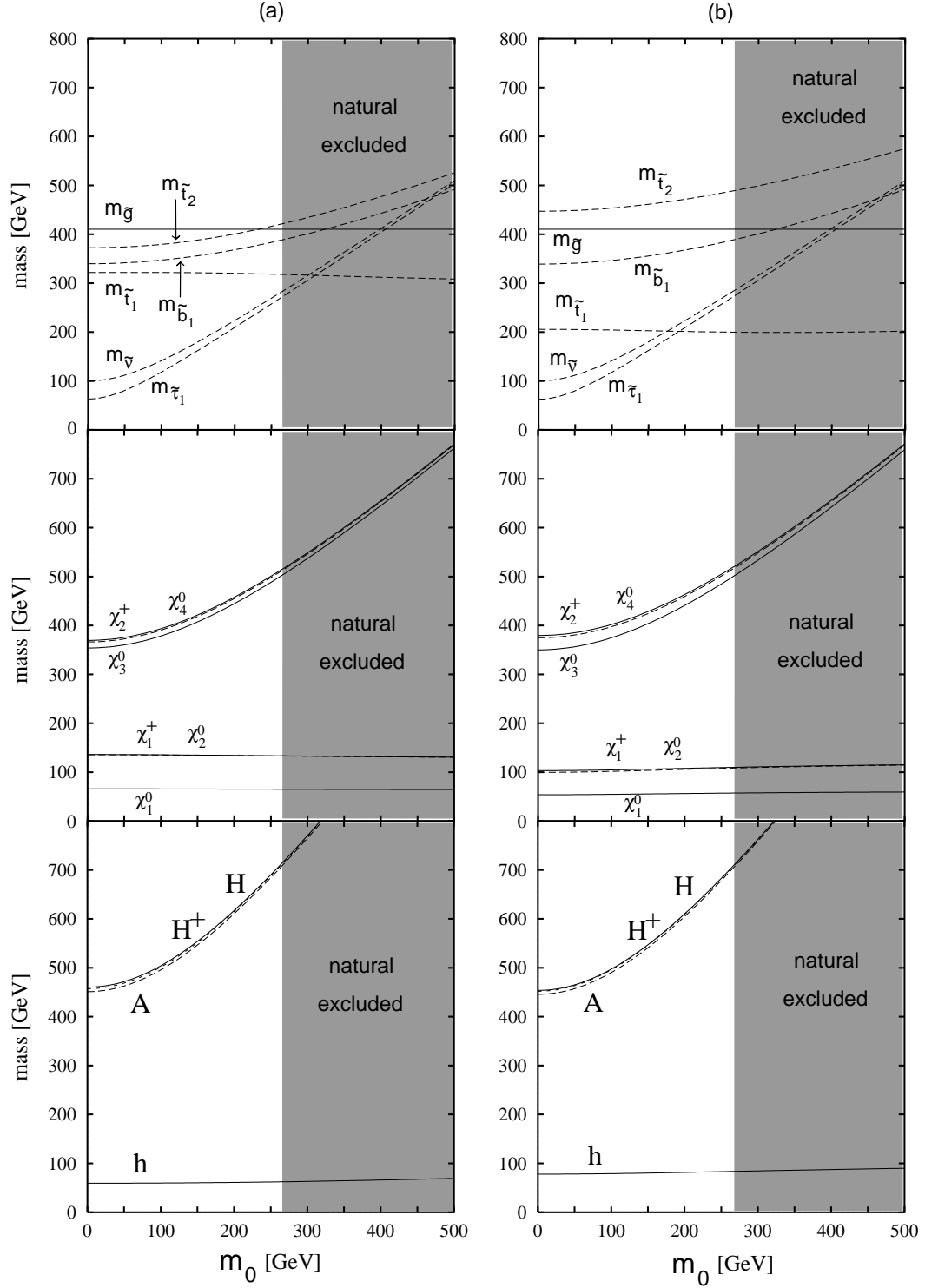


Fig. 9. The low  $\tan\beta$  fixed point solutions for (a)  $\mu > 0$  and (b)  $\mu < 0$  with  $m_{\frac{1}{2}} = 150$  GeV and  $A^G = 0$ . The shaded area denotes the region excluded by our naturalness criterion.

We also give qualitative descriptions of the allowed parameter space in the other significant  $m_t - \tan \beta$  regions.

- **(b) Medium-tan  $\beta$  Fixed Point**

The allowed  $m_0 - m_{\frac{1}{2}}$  parameter space is substantially larger in this case than it is for the low-tan  $\beta$  fixed point. Our naturalness condition allows substantially larger values of  $m_0$  and  $m_{\frac{1}{2}}$  ( $m_0 \lesssim 725$  GeV and  $m_{\frac{1}{2}} \lesssim 325$  GeV for  $m_t(m_t) = 192$  GeV, and  $\tan \beta = 15$ ); however, dark matter constraints will still require  $m_0 \lesssim 300$  GeV. For  $\mu > 0$ , experimental bounds on  $m_{\tilde{\nu}}$ ,  $m_{\tilde{\tau}_1}$ , and  $m_{\chi_{1\pm}}$  push the lower bound for  $m_0$  and  $m_{\frac{1}{2}}$  up slightly. For  $\mu < 0$ , experimental bounds for  $m_{\tilde{\nu}}$  and  $m_{\tilde{\tau}_1}$  also become more restrictive, but the  $m_{\chi_{1\pm}}$  and  $m_{\tilde{t}_1}$  constraints become less restrictive. In both cases the constraint from the lightest scalar higgs mass becomes less restrictive; even in the  $\mu > 0$  case, it will not play an important role in limiting the allowed  $m_0$  and  $m_{\frac{1}{2}}$  region. To summarize, the medium-tan  $\beta$  fixed point region allows larger values of  $m_0$  and  $m_{\frac{1}{2}}$  from our naturalness constraint while the experimental restrictions on this parameter space do not change much from the low-tan  $\beta$  case.

- **(c) High-tan  $\beta$  Fixed Point**

This region describes the SO(10) relation  $\lambda_t = \lambda_b = \lambda_\tau$  where  $\lambda_i \gtrsim 1$ . There is not much parameter space remaining without weakening our naturalness condition. For the case  $m_t(m_t) = 178$  GeV,  $\tan \beta = 61$  (with  $m_0 = 400$  GeV,  $m_{\frac{1}{2}} = 400$  GeV, and  $\mu(m_t) \approx 575$  GeV) the particle spectrum is given in the

following table.

Particle	Mass (GeV)
gluino	1078
stop, sbottom	751,900; 763,881
up squarks, down squarks	1029,1060; 1026,1063
stau, tau sneutrino	183,454; 417
other sleptons	431,494; 487
charginos	323,590
neutralinos	167,323,579,588
higgs: $m_A, m_{H^\pm}, m_H, m_h$	364,377,363,131

**Table 3:** Particle spectrum for  $m_t = 178$  GeV,  $\tan \beta = 61$

(where  $m_0 = 400$  GeV,  $m_{\frac{1}{2}} = 400$  GeV,  $A^G = 0$ ).

As before the above particle spectrum is calculated at the scale  $m_t$ . We obtain no natural solutions for  $\mu < 0$ .

- **(d) Low- $\tan \beta$ , not a Fixed Point**

This region has a large amount of viable parameter space; naturalness bounds allow substantially higher values of  $m_{\frac{1}{2}}$  ( $m_{\frac{1}{2}} \lesssim 330$  GeV for  $m_t(m_t) = 160$  GeV with  $\tan \beta = 3$ ), and experimental constraints do not further restrict this parameter space to any great extent (though the sneutrino and chargino bounds are pushed upward somewhat). In fact, the higgs constraint is weakened a great deal for  $\mu > 0$ , allowing relatively low values for  $m_0$  and  $m_{\frac{1}{2}}$ . Moreover, the light stop constraint is less important in the  $\mu < 0$  case.

- **(e) High- $\tan\beta$ , not a Fixed Point**

The allowed parameter space is reduced by the lightest stau constraint (which cannot be the LSP), though some parameter region remains. The allowed parameter space is bounded by chargino, stau, dark matter, and our naturalness constraint which give  $180 \lesssim m_0 \lesssim 300$  GeV and  $85 \lesssim m_{\frac{1}{2}} \lesssim 400$  GeV for  $m_t(m_t) = 160$  GeV,  $\tan\beta = 45$ . The light higgs and the light stop constraints are not important for either sign of  $\mu$ .

In addition, we varied  $A^G$  from  $-500$  to  $+500$  GeV in the low  $\tan\beta$  fixed point case; we found little change in the resulting parameter space except that the light stop constraint is more (less) restrictive for  $A^G$  negative (positive) and  $\mu < 0$ . The fixed point solution in radiative electroweak symmetry breaking has also been studied recently in Ref. [13].

A critical constraint[43, 47, 48] on the supersymmetric spectrum is the rare decay  $b \rightarrow s\gamma$ . We remark here that regions of the parameter space illustrated in the previous figures are not ruled out by this constraint. This will be the subject of a forthcoming paper[49].

## 8 SUSY Mass Spectrum Correlations

For smaller values of  $\tan\beta$  it is clear from the tree-level expression Eq. (22) that  $|\mu|$  is usually large compared to the the electroweak scale  $M_Z$ . Furthermore the fine-tuning problem in this situation is softened when the one-loop contributions to the Higgs potential are included. For values of  $\mu$  just a few times larger than  $M_Z$ , the



particle spectrum is governed by certain asymptotic behaviors which we discuss in this section.

As discussed previously, the gaugino masses are related (through one-loop order) by the same ratios that describe the gauge couplings at the electroweak scale. This observation, together with the fact that  $|\mu|$  is large, yields simple correlations between the lightest chargino and neutralinos and the gluino[7, 50], namely

$$M_{\chi_1^0} \simeq M_1, \quad (41a)$$

$$M_{\chi_1^\pm} \simeq M_{\chi_2^0} \simeq M_2 = \frac{\alpha_2}{\alpha_1} M_1 \simeq 2M_1 \simeq M_{\chi_1^0}, \quad (41b)$$

$$m_{\tilde{g}} = M_3 = \frac{\alpha_3}{\alpha_2} M_2 = \frac{\alpha_3}{\alpha_1} M_1, \quad (41c)$$

where the quantities in these equations are evaluated at scale  $m_t$ . The heaviest chargino and the two heaviest neutralino states are primarily Higgsino with

$$M_{\chi_2^\pm} \simeq M_{\chi_3^0} \simeq M_{\chi_4^0} \simeq |\mu|. \quad (42)$$

$$(43)$$

The lightest Higgs  $h$  has small mass for  $\tan \beta$  near one at tree-level by virtue of the D-flat direction; its mass comes from radiative corrections[24, 51]. The heavy Higgs states are (approximately) degenerate  $\approx M_A$  because at tree-level  $M_A = -\frac{B\mu}{\sin 2\beta} \approx -B\mu$  is large.

The squark and slepton masses also display simple asymptotic behavior at large  $|\mu|$ . The first and second squark generations are approximately degenerate (though not degenerate enough to ignore their contributions to the minimization of the effective potential). The squark and slepton mass spectra are shown in Figures 7 through

9. The splitting of the stop quark masses grows as  $|\mu|$  increases. This splitting of the sbottom states does not change much with  $\mu$  for small  $\tan\beta$ .

## 9 Dark Matter

The neutralino as the LSP is an ideal candidate for the dark matter since it is stable and interacts weakly. The MSSM utilizes R-parity conservation so the lightest neutralino must annihilate to ordinary matter ( $\chi\chi \rightarrow \text{R-even matter}$ ) to a sufficient extent to avoid overclosing the universe[52]. For a bino-like LSP, dark matter considerations put an upper bound on the parameter  $m_0$ . We adopt the conservative viewpoint that the contribution of the LSP alone to the dark matter of the universe must be less than the closure density. Roberts and Roszkowski[53] apply an additional constraint in which the neutralino is required to make up a substantial fraction of the dark matter; this requirement provides a lower bound on  $m_0$  as well. The recent results from COBE suggest that the dark matter is a mixture of hot and cold dark matter. Although it may be simpler to assume that all of the cold dark matter is composed of one contribution, it is perhaps premature to assume this. We remark that the recent exciting claims of experimental evidence for dark matter in nearby galaxies[54, 55] only solves the local baryonic dark matter problem[56]. The origin of the nonbaryonic dark matter needed to close the universe is still unknown.

The typical situation in the low  $\tan\beta$  fixed point solutions is that  $|\mu| \gg M_2$  and consequently the lightest neutralino (which is the LSP) is predominantly gaugino;

indeed the LSP is predominantly bino. The neutralino mass matrix is

$$M_N = \begin{pmatrix} M_1 & 0 & -M_Z \cos \beta \sin \theta_W & M_Z \sin \beta \sin \theta_W \\ 0 & M_2 & M_Z \cos \beta \cos \theta_W & -M_Z \sin \beta \cos \theta_W \\ -M_Z \cos \beta \sin \theta_W & M_Z \cos \beta \cos \theta_W & 0 & \mu \\ M_Z \sin \beta \sin \theta_W & -M_Z \sin \beta \cos \theta_W & \mu & 0 \end{pmatrix}. \quad (44)$$

For  $|\mu| \gg M_2$  the lightest two neutralinos are predominantly bino and wino, and hence the bino and gaugino purities are high. In this case any mass limit on the lightest neutralino from  $Z$  decays at LEP disappears since the  $Z$  couples only to the Higgsino component of the neutralino. Figure 10 gives the bino and gaugino purities for the low- $\tan \beta$  fixed point solution in the no-scale model, corresponding to Fig. 7.

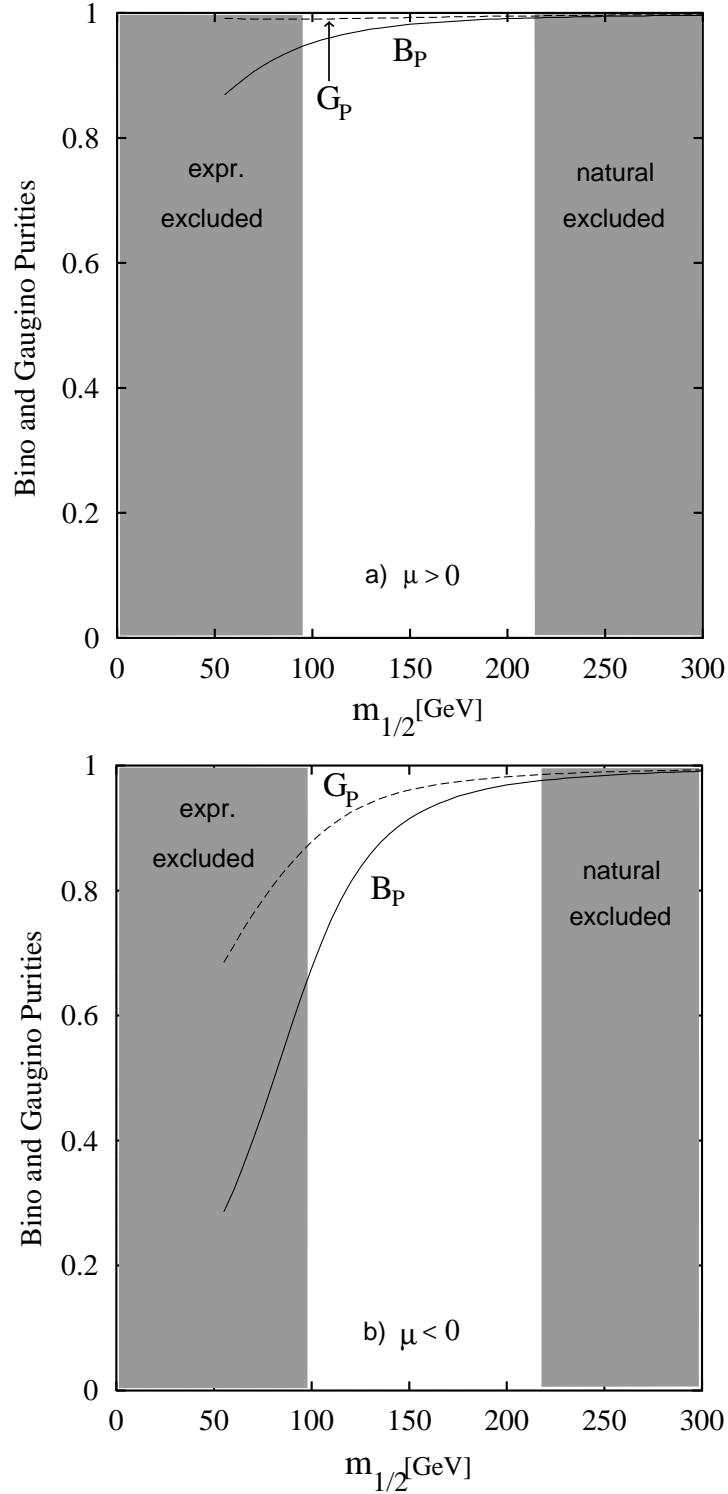


Fig. 10. The bino and gaugino purities for the low  $\tan\beta$  fixed point solution with  $m_t = 160$  GeV,  $\tan\beta = 1.47$  in the no-scale model with (a)  $\mu > 0$  and (b)  $\mu < 0$ . Shaded regions are forbidden by experimental and fine-tuning considerations.

Given that the solutions are comfortably in the high bino purity region, we apply the semi-quantitative constraint of Drees and Nojiri[46] (valid roughly for  $|\mu| > m_{\frac{1}{2}}$ ,  $M_{\chi_1^0} > 60$  GeV)

$$\frac{(m_0^2 + 1.83M_{\chi_1^0}^2)^2}{M_{\chi_1^0}^2 \left[ \left( 1 - \frac{M_{\chi_1^0}^2}{m_0^2 + 1.83M_{\chi_1^0}^2} \right)^2 + \left( \frac{M_{\chi_1^0}^2}{m_0^2 + 1.83M_{\chi_1^0}^2} \right)^2 \right]} < 1 \times 10^6 \text{ GeV}^2, \quad (45)$$

to obtain the line corresponding to  $\Omega h^2 = 1$  in Figure 6. This formula is based on the observation that for the bino-like LSP the annihilation rate is dominated by the sleptons, and it neglects a possible enhanced annihilation rate that may occur if there are significant  $s$ -channel pole contributions. The bino and gaugino purities for non-zero  $m_0$  (in particular the dilaton model) are similar to the above figures.

## 10 Conclusion

The motivation of this work has been to distill the interesting supersymmetric phenomenology of the low-tan  $\beta$  fixed-point region that can explain the origin of a large top quark mass. The RGEs are solved with some boundary conditions taken from both GUT and low energy scales. The minimization conditions on the effective potential are obtained with the tadpole method.

Our principle findings can be summarized as follows:

- Solutions with a  $\lambda_t$  fixed point,  $m_t \lesssim 170$  GeV and radiative breaking of the electroweak symmetry breaking are allowed. These solutions are characterized by relatively large values of the supersymmetric Higgs mass parameter  $|\mu|$ , which implies that the supersymmetric particle spectrum displays a simple asymptotic

behavior. The solutions also meet the naturalness criterion  $|\mu(M_Z)| < 500$  GeV for both signs of  $\mu$ .

- Representative sparticle mass spectra are presented for the  $\lambda_t$  fixed point solutions.
- Over most of the GUT parameter space for the low-tan  $\beta$  fixed-point, the gaugino masses exhibit show simple correlations due to the relatively large value  $|\mu|$  compared to  $M_2$ . The heaviest chargino and the two heaviest neutralinos have masses approximately  $|\mu|$ ; the lightest chargino and the second lightest neutralino have masses approximately  $M_2$ ; the lightest neutralino (LSP) has a mass approximately  $M_1 \simeq M_2/2$ . The lightest Higgs obtains its mass almost entirely from radiative corrections, and the states  $H, H^\pm, A$  are relatively heavy and approximately degenerate.
- In the early universe the LSP will annihilate sufficiently neglecting  $s$ -channel pole annihilation for most of the parameter space ( $m_0 \lesssim 300$  GeV) so as not to overclose the universe.
- The values of  $\mu$  and  $B$  derived from the one-loop Higgs potential analyses are very similar to the tree-level results in the low-tan  $\beta$  fixed-point region when the parameters  $M_Z$  and  $\tan \beta$  are taken as input. However, the one-loop corrections to the Higgs potential somewhat ameliorate the fine-tuning problem.
- The tadpole method is a convenient way to calculate the one-loop minimization conditions. We have obtained these conditions in an analytic form including all

contributions from the gauge-Higgs sector and matter multiplets.

## 11 Acknowledgements

We thank Manuel Drees for a discussion on dark matter and Roger Phillips for collaboration on  $b \rightarrow s\gamma$  analyses. PO would like to thank Chris Kolda for discussions regarding supersymmetric model building. This research was supported in part by the University of Wisconsin Research Committee with funds granted by the Wisconsin Alumni Research Foundation, in part by the U.S. Department of Energy under contract no. DE-AC02-76ER00881, and in part by the Texas National Laboratory Research Commission under grant nos. RGFY93-221 and FCFY9302. MSB was supported in part by an SSC Fellowship. PO was supported in part by an NSF Graduate Fellowship.

## 12 Appendix

### Renormalization Group Equations

The renormalization equations for the gauge couplings and the Yukawa couplings to two-loop order can be found in Ref. [15]. In the most general case the evolution equations involve matrices. For example the Yukawa couplings form three-by-three Yukawa matrices:  $\mathbf{U}$  for the up-type quarks,  $\mathbf{D}$  for the down-type quarks, and  $\mathbf{E}$  for the charged leptons. Similarly the soft-supersymmetry breaking parameters form the matrices  $\mathbf{M}_{Q_L}$ ,  $\mathbf{M}_{U_R}$ ,  $\mathbf{M}_{D_R}$ ,  $\mathbf{M}_{L_L}$ , and  $\mathbf{M}_{E_R}$ . Finally there are in general matrices for the trilinear soft-supersymmetry breaking ‘‘A-terms’’:  $\mathbf{A}_U$ ,  $\mathbf{A}_D$ , and  $\mathbf{A}_E$ . It turns out to be useful to define the combinations  $\mathbf{U}_{\mathbf{A}ij} \equiv \mathbf{A}_{Uij} \mathbf{U}_{ij}$ , etc. in the matrix version of the RGE’s. Then the evolution of the soft-supersymmetry parameters (with our convention for signs) is given by the following renormalization group equations[47]

$$\frac{dM_i}{dt} = \frac{2}{16\pi^2} b_i g_i^2 M_i, \quad (46a)$$

$$\begin{aligned} \frac{d\mathbf{U}_A}{dt} = & \frac{1}{16\pi^2} \left[ - \left( \frac{13}{15} g_1^2 + 3g_2^2 + \frac{16}{3} g_3^2 \right) \mathbf{U}_A + 2 \left( \frac{13}{15} g_1^2 M_1 + 3g_2^2 M_2 + \frac{16}{3} g_3^2 M_3 \right) \mathbf{U} \right. \\ & + \left\{ 4(\mathbf{U}_A \mathbf{U}^\dagger \mathbf{U}) + 6\text{Tr}(\mathbf{U}_A \mathbf{U}^\dagger) \mathbf{U} \right\} + \left\{ 5(\mathbf{U} \mathbf{U}^\dagger \mathbf{U}_A) + 3\text{Tr}(\mathbf{U} \mathbf{U}^\dagger) \mathbf{U}_A \right\} \\ & \left. + 2(\mathbf{D}_A \mathbf{D}^\dagger \mathbf{U}) + (\mathbf{D} \mathbf{D}^\dagger \mathbf{U}_A) \right\}, \quad (46b) \end{aligned}$$

$$\begin{aligned} \frac{d\mathbf{D}_A}{dt} = & \frac{1}{16\pi^2} \left[ - \left( \frac{7}{15} g_1^2 + 3g_2^2 + \frac{16}{3} g_3^2 \right) \mathbf{D}_A + 2 \left( \frac{7}{15} g_1^2 M_1 + 3g_2^2 M_2 + \frac{16}{3} g_3^2 M_3 \right) \mathbf{D} \right. \\ & + \left\{ 4(\mathbf{D}_A \mathbf{D}^\dagger \mathbf{D}) + 6\text{Tr}(\mathbf{D}_A \mathbf{D}^\dagger) \mathbf{D} \right\} + \left\{ 5(\mathbf{D} \mathbf{D}^\dagger \mathbf{D}_A) + 3\text{Tr}(\mathbf{D} \mathbf{D}^\dagger) \mathbf{D}_A \right\} \\ & \left. + 2(\mathbf{U}_A \mathbf{U}^\dagger \mathbf{D}) + (\mathbf{U} \mathbf{U}^\dagger \mathbf{D}_A) + 2\text{Tr}(\mathbf{E}_A \mathbf{E}^\dagger) \mathbf{D} + \text{Tr}(\mathbf{E} \mathbf{E}^\dagger) \mathbf{D}_A \right\}, \quad (46c) \end{aligned}$$

$$\frac{d\mathbf{E}_A}{dt} = \frac{1}{16\pi^2} \left[ - (3g_1^2 + 3g_2^2) \mathbf{E}_A + 2(3g_1^2 M_1 + 3g_2^2 M_2) \mathbf{E} \right]$$



$$\begin{aligned}
& + \left\{ \left[ 4(\mathbf{E}_A \mathbf{E}^\dagger \mathbf{E}) + 2\text{Tr}(\mathbf{E}_A \mathbf{E}^\dagger) \mathbf{E} \right] + \left[ 5(\mathbf{E} \mathbf{E}^\dagger \mathbf{E}_A) + \text{Tr}(\mathbf{E} \mathbf{E}^\dagger) \mathbf{E}_A \right] \right. \\
& \left. + 6(\mathbf{D}_A \mathbf{D}^\dagger \mathbf{E}) + 3(\mathbf{D} \mathbf{D}^\dagger \mathbf{E}_A) \right\} , \tag{46d}
\end{aligned}$$

$$\frac{dB}{dt} = \frac{2}{16\pi^2} \left( \frac{3}{5} g_1^2 M_1 + 3g_2^2 M_2 + \text{Tr}(3\mathbf{U} \mathbf{U}_A + 3\mathbf{D} \mathbf{D}_A + \mathbf{E} \mathbf{E}_A) \right) , \tag{46e}$$

$$\frac{d\mu}{dt} = \frac{\mu}{16\pi^2} \left( -\frac{3}{5} g_1^2 - 3g_2^2 + \text{Tr}(3\mathbf{U} \mathbf{U}^\dagger + 3\mathbf{D} \mathbf{D}^\dagger + \mathbf{E} \mathbf{E}^\dagger) \right) , \tag{46f}$$

$$\begin{aligned}
\frac{dM_{H_1}^2}{dt} &= \frac{2}{16\pi^2} \left( -\frac{3}{5} g_1^2 M_1^2 - 3g_2^2 M_2^2 \right. \\
&+ 3\text{Tr}(\mathbf{D}(\mathbf{M}_{Q_L}^2 + \mathbf{M}_{D_R}^2) \mathbf{D}^\dagger + M_{H_1}^2 \mathbf{D} \mathbf{D}^\dagger + \mathbf{D}_A \mathbf{D}_A^\dagger) \\
&+ \left. \text{Tr}(\mathbf{E}(\mathbf{M}_{L_L}^2 + \mathbf{M}_{E_R}^2) \mathbf{E}^\dagger + M_{H_1}^2 \mathbf{E} \mathbf{E}^\dagger + \mathbf{E}_A \mathbf{E}_A^\dagger) \right) , \tag{46g}
\end{aligned}$$

$$\begin{aligned}
\frac{dM_{H_2}^2}{dt} &= \frac{2}{16\pi^2} \left( -\frac{3}{5} g_1^2 M_1^2 - 3g_2^2 M_2^2 \right. \\
&+ \left. 3\text{Tr}(\mathbf{U}(\mathbf{M}_{Q_L}^2 + \mathbf{M}_{U_R}^2) \mathbf{U}^\dagger + M_{H_2}^2 \mathbf{U} \mathbf{U}^\dagger + \mathbf{U}_A \mathbf{U}_A^\dagger) \right) , \tag{46h}
\end{aligned}$$

$$\begin{aligned}
\frac{d\mathbf{M}_{Q_L}^2}{dt} &= \frac{2}{16\pi^2} \left( -\frac{1}{15} g_1^2 M_1^2 - 3g_2^2 M_2^2 - \frac{16}{3} g_3^2 M_3^2 \right. \\
&+ \frac{1}{2} [\mathbf{U} \mathbf{U}^\dagger \mathbf{M}_{Q_L}^2 + \mathbf{M}_{Q_L}^2 \mathbf{U} \mathbf{U}^\dagger + 2(\mathbf{U} \mathbf{M}_{U_R}^2 \mathbf{U}^\dagger + m_{H_2}^2 \mathbf{U} \mathbf{U}^\dagger + \mathbf{U}_A \mathbf{U}_A^\dagger)] \\
&+ \left. \frac{1}{2} [\mathbf{D} \mathbf{D}^\dagger \mathbf{M}_{Q_L}^2 + \mathbf{M}_{Q_L}^2 \mathbf{D} \mathbf{D}^\dagger + 2(\mathbf{D} \mathbf{M}_{D_R}^2 \mathbf{D}^\dagger + m_2^2 \mathbf{D} \mathbf{D}^\dagger + \mathbf{D}_A \mathbf{D}_A^\dagger)] \right) , \tag{46i}
\end{aligned}$$

$$\begin{aligned}
\frac{d\mathbf{M}_{U_R}^2}{dt} &= \frac{2}{16\pi^2} \left( -\frac{16}{15} g_1^2 M_1^2 - \frac{16}{3} g_3^2 M_3^2 \right. \\
&+ \left. [\mathbf{U}^\dagger \mathbf{U} \mathbf{M}_{U_R}^2 + \mathbf{M}_{U_R}^2 \mathbf{U}^\dagger \mathbf{U} + 2(\mathbf{U}^\dagger \mathbf{M}_{Q_L}^2 \mathbf{U} + m_{H_2}^2 \mathbf{U}^\dagger \mathbf{U} + \mathbf{U}_A^\dagger \mathbf{U}_A)] \right) , \tag{46j}
\end{aligned}$$

$$\begin{aligned}
\frac{d\mathbf{M}_{D_R}^2}{dt} &= \frac{2}{16\pi^2} \left( -\frac{4}{15} g_1^2 M_1^2 - \frac{16}{3} g_3^2 M_3^2 \right. \\
&+ \left. [\mathbf{D}^\dagger \mathbf{D} \mathbf{M}_{D_R}^2 + \mathbf{M}_{D_R}^2 \mathbf{D}^\dagger \mathbf{D} + 2(\mathbf{D}^\dagger \mathbf{M}_{Q_L}^2 \mathbf{D} + m_{H_1}^2 \mathbf{D}^\dagger \mathbf{D} + \mathbf{D}_A^\dagger \mathbf{D}_A)] \right) , \tag{46k}
\end{aligned}$$

$$\begin{aligned}
\frac{d\mathbf{M}_{L_L}^2}{dt} &= \frac{2}{16\pi^2} \left( -\frac{3}{5} g_1^2 M_1^2 - 3g_2^2 M_2^2 \right. \\
&+ \left. \frac{1}{2} [\mathbf{E} \mathbf{E}^\dagger \mathbf{M}_{L_L}^2 + \mathbf{M}_{L_L}^2 \mathbf{E} \mathbf{E}^\dagger + 2(\mathbf{E} \mathbf{M}_{E_R}^2 \mathbf{E}^\dagger + m_{H_1}^2 \mathbf{E} \mathbf{E}^\dagger + \mathbf{E}_A \mathbf{E}_A^\dagger)] \right) , \tag{46l}
\end{aligned}$$

$$\begin{aligned}
\frac{d\mathbf{M}_{E_R}^2}{dt} &= \frac{2}{16\pi^2} \left( -\frac{12}{5} g_1^2 M_1^2 \right. \\
&+ \left. [\mathbf{E}^\dagger \mathbf{E} \mathbf{M}_{E_R}^2 + \mathbf{M}_{E_R}^2 \mathbf{E}^\dagger \mathbf{E} + 2(\mathbf{E}^\dagger \mathbf{M}_{L_L}^2 \mathbf{E} + m_{H_1}^2 \mathbf{E}^\dagger \mathbf{E} + \mathbf{E}_A^\dagger \mathbf{E}_A)] \right) , \tag{46m}
\end{aligned}$$

For our purposes it is sufficient to consider these equations keeping only the leading terms in the mass hierarchy in the three generation MSSM. The resulting renormalization group equations[57] are given below to leading order.

$$\frac{dM_i}{dt} = \frac{2}{16\pi^2} b_i g_i^2 M_i, \quad (47a)$$

$$\frac{dA_t}{dt} = \frac{2}{16\pi^2} \left( \sum c_i g_i^2 M_i + 6\lambda_t^2 A_t + \lambda_b^2 A_b \right), \quad (47b)$$

$$\frac{dA_b}{dt} = \frac{2}{16\pi^2} \left( \sum c'_i g_i^2 M_i + 6\lambda_b^2 A_b + \lambda_t^2 A_t + \lambda_\tau^2 A_\tau \right), \quad (47c)$$

$$\frac{dA_\tau}{dt} = \frac{2}{16\pi^2} \left( \sum c''_i g_i^2 M_i + 3\lambda_b^2 A_b + 4\lambda_\tau^2 A_\tau \right), \quad (47d)$$

$$\frac{dB}{dt} = \frac{2}{16\pi^2} \left( \frac{3}{5} g_1^2 M_1 + 3g_2^2 M_2 + 3\lambda_b^2 A_b + 3\lambda_t^2 A_t + \lambda_\tau^2 A_\tau \right), \quad (47e)$$

$$\frac{d\mu}{dt} = \frac{\mu}{16\pi^2} \left( -\frac{3}{5} g_1^2 - 3g_2^2 + 3\lambda_t^2 + 3\lambda_b^2 + \lambda_\tau^2 \right), \quad (47f)$$

$$\frac{dM_{H_1}^2}{dt} = \frac{2}{16\pi^2} \left( -\frac{3}{5} g_1^2 M_1^2 - 3g_2^2 M_2^2 + 3\lambda_b^2 X_b + \lambda_\tau^2 X_\tau \right), \quad (47g)$$

$$\frac{dM_{H_2}^2}{dt} = \frac{2}{16\pi^2} \left( -\frac{3}{5} g_1^2 M_1^2 - 3g_2^2 M_2^2 + 3\lambda_t^2 X_t \right), \quad (47h)$$

$$\frac{dM_{Q_L}^2}{dt} = \frac{2}{16\pi^2} \left( -\frac{1}{15} g_1^2 M_1^2 - 3g_2^2 M_2^2 - \frac{16}{3} g_3^2 M_3^2 + \lambda_t^2 X_t + \lambda_b^2 X_b \right), \quad (47i)$$

$$\frac{dM_{t_R}^2}{dt} = \frac{2}{16\pi^2} \left( -\frac{16}{15} g_1^2 M_1^2 - \frac{16}{3} g_3^2 M_3^2 + 2\lambda_t^2 X_t \right), \quad (47j)$$

$$\frac{dM_{b_R}^2}{dt} = \frac{2}{16\pi^2} \left( -\frac{4}{15} g_1^2 M_1^2 - \frac{16}{3} g_3^2 M_3^2 + 2\lambda_b^2 X_b \right), \quad (47k)$$

$$\frac{dM_{L_L}^2}{dt} = \frac{2}{16\pi^2} \left( -\frac{3}{5} g_1^2 M_1^2 - 3g_2^2 M_2^2 + \lambda_\tau^2 X_\tau \right), \quad (47l)$$

$$\frac{dM_{\tau_R}^2}{dt} = \frac{2}{16\pi^2} \left( -\frac{12}{5} g_1^2 M_1^2 + 2\lambda_\tau^2 X_\tau \right), \quad (47m)$$

and for the two light generations,

$$\frac{dA_u}{dt} = \frac{2}{16\pi^2} \left( \sum c_i g_i^2 M_i + \lambda_t^2 A_t \right), \quad (48a)$$

$$\frac{dA_d}{dt} = \frac{2}{16\pi^2} \left( \sum c'_i g_i^2 M_i + \lambda_b^2 A_b + \frac{1}{3} \lambda_\tau^2 A_\tau \right), \quad (48b)$$

$$\frac{dA_e}{dt} = \frac{2}{16\pi^2} \left( \sum c''_i g_i^2 M_i + \lambda_b^2 A_b + \frac{1}{3} \lambda_\tau^2 A_\tau \right), \quad (48c)$$

$$\frac{dM_{q_L}^2}{dt} = \frac{2}{16\pi^2} \left( -\frac{1}{15}g_1^2M_1^2 - 3g_2^2M_2^2 - \frac{16}{3}g_3^2M_3^2 \right), \quad (48d)$$

$$\frac{dM_{u_R}^2}{dt} = \frac{2}{16\pi^2} \left( -\frac{16}{15}g_1^2M_1^2 - \frac{16}{3}g_3^2M_3^2 \right), \quad (48e)$$

$$\frac{dM_{d_R}^2}{dt} = \frac{2}{16\pi^2} \left( -\frac{4}{15}g_1^2M_1^2 - \frac{16}{3}g_3^2M_3^2 \right), \quad (48f)$$

$$\frac{dM_{l_L}^2}{dt} = \frac{2}{16\pi^2} \left( -\frac{3}{5}g_1^2M_1^2 - 3g_2^2M_2^2 \right), \quad (48g)$$

$$\frac{dM_{e_R}^2}{dt} = \frac{2}{16\pi^2} \left( -\frac{12}{5}g_1^2M_1^2 \right), \quad (48h)$$

where

$$b_i = \left( \frac{33}{5}, 1, -3 \right), \quad (49a)$$

$$c_i = \left( \frac{13}{15}, 3, \frac{16}{3} \right), \quad (49b)$$

$$c'_i = \left( \frac{7}{15}, 3, \frac{16}{3} \right), \quad (49c)$$

$$c''_i = \left( \frac{9}{5}, 3, 0 \right), \quad (49d)$$

$$X_t = M_{Q_L}^2 + M_{t_R}^2 + M_{H_2}^2 + A_t^2, \quad (49e)$$

$$X_b = M_{Q_L}^2 + M_{b_R}^2 + M_{H_1}^2 + A_b^2, \quad (49f)$$

$$X_\tau = M_{L_L}^2 + M_{\tau_R}^2 + M_{H_1}^2 + A_\tau^2. \quad (49g)$$

Here the factors  $c_i$ ,  $c'_i$ , and  $c''_i$  are given by a sum over the fields in the relevant Yukawa coupling, e.g.  $c_i = \sum_f c_i(f) = c_i(H_2) + c_i(Q) + c_i(U^c)$ . The coefficients in front of the gauge coupling parts of Eq. (41)-(43) can be understood from the quantum numbers. For the fundamental representations of  $SU(N)$  there is a factor of  $(N^2 - 1)/N$  and for the hypercharge  $U(1)$  one has  $\frac{3}{10}Y^2$  (with hypercharge suitably normalized, e.g.  $Y_{\tau_R} = 2$ ).

## One-Loop Effective Potential

We summarize here the tools needed to construct the one-loop minimization conditions. The necessary ingredients are the field dependent particle masses; since we are calculating the tadpole diagrams, we need the particle masses at the potential minimum and the Higgs couplings. The tadpoles are calculated in the  $\overline{DR}$  renormalization scheme[25].

We present here the contribution from the third generation (s)particles; the contributions from the other generations can be obtained with obvious substitutions. The top and bottom squark and the tau slepton mass matrices (at the potential minimum) are

$$\left( \begin{array}{cc} M_{QL}^2 + m_t^2 + \frac{1}{6}(4M_W^2 - M_Z^2) \cos 2\beta & m_t(A_t + \mu \cot \beta) \\ m_t(A_t + \mu \cot \beta) & M_{tR}^2 + m_t^2 - \frac{2}{3}(M_W^2 - M_Z^2) \cos 2\beta \end{array} \right), \quad (50a)$$

$$\left( \begin{array}{cc} M_{QL}^2 + m_b^2 - \frac{1}{6}(2M_W^2 + M_Z^2) \cos 2\beta & m_b(A_b + \mu \tan \beta) \\ m_b(A_b + \mu \tan \beta) & M_{bR}^2 + m_b^2 + \frac{1}{3}(M_W^2 - M_Z^2) \cos 2\beta \end{array} \right), \quad (50b)$$

$$\left( \begin{array}{cc} M_{LL}^2 + m_\tau^2 - \frac{1}{2}(2M_W^2 - M_Z^2) \cos 2\beta & m_\tau(A_\tau + \mu \tan \beta) \\ m_\tau(A_\tau + \mu \tan \beta) & M_{\tau R}^2 + m_\tau^2 + (M_W^2 - M_Z^2) \cos 2\beta \end{array} \right), \quad (50c)$$

which are diagonalized by orthogonal matrices with mixing angles  $\theta_{\tilde{t}}$ ,  $\theta_{\tilde{b}}$ , and  $\theta_{\tilde{\tau}}$ . The mass eigenstate for the massive third generation sneutrino is

$$m_{\tilde{\nu}}^2 = M_{LL}^2 + \frac{1}{2}M_Z^2 \cos 2\beta. \quad (51a)$$

The relevant Higgs couplings to the squark eigenstates are

$$\left\{ \begin{array}{l} V(\mathcal{J}\tilde{t}_1\tilde{t}_1) \\ V(\mathcal{J}\tilde{t}_2\tilde{t}_2) \end{array} \right\} = \frac{igm_t^2}{M_W^2} \pm \frac{igm_t}{2M_W} \sin 2\theta_t [A_t - \mu \cot \beta] - \frac{igM_Z}{\cos \theta_W} \left[ \left\{ \begin{array}{l} \cos^2 \theta_t \\ \sin^2 \theta_t \end{array} \right\} \left( \frac{1}{2} - e_t \sin^2 \theta_W \right) + \left\{ \begin{array}{l} \sin^2 \theta_t \\ \cos^2 \theta_t \end{array} \right\} (e_t \sin^2 \theta_W) \right], \quad (52a)$$

$$\left\{ \begin{array}{l} V(\mathcal{J}_\perp\tilde{t}_1\tilde{t}_1) \\ V(\mathcal{J}_\perp\tilde{t}_2\tilde{t}_2) \end{array} \right\} = -\frac{igm_t^2}{M_W^2} \cot \beta \mp \frac{igm_t}{2M_W} \sin 2\theta_t [A_t + \mu \tan \beta], \quad (52b)$$

$$\left\{ \begin{array}{l} V(\mathcal{J}\tilde{b}_1\tilde{b}_1) \\ V(\mathcal{J}\tilde{b}_2\tilde{b}_2) \end{array} \right\} = \frac{igm_b^2}{M_W^2} \mp \frac{igm_b}{2M_W} \sin 2\theta_b [A_b - \mu \tan \beta]$$

$$+ \frac{igM_Z}{\cos\theta_W} \left[ \left\{ \begin{array}{c} \cos^2\theta_b \\ \sin^2\theta_b \end{array} \right\} \left( \frac{1}{2} + e_b \sin^2\theta_W \right) + \left\{ \begin{array}{c} \sin^2\theta_b \\ \cos^2\theta_b \end{array} \right\} (e_b \sin^2\theta_W) \right], \quad (52c)$$

$$\left\{ \begin{array}{c} V(\mathcal{J}_\perp \tilde{b}_1 \tilde{b}_1) \\ V(\mathcal{J}_\perp \tilde{b}_2 \tilde{b}_2) \end{array} \right\} = -\frac{igm_b^2}{M_W^2} \tan\beta \mp \frac{igm_b}{2M_W} \sin 2\theta_b [A_b \tan\beta + \mu], \quad (52d)$$

$$\left\{ \begin{array}{c} V(\mathcal{J} \tilde{\tau}_1 \tilde{\tau}_1) \\ V(\mathcal{J} \tilde{\tau}_2 \tilde{\tau}_2) \end{array} \right\} = \frac{igm_\tau^2}{M_W^2} \mp \frac{igm_\tau}{2M_W} \sin 2\theta_\tau [A_\tau - \mu \tan\beta] \\ + \frac{igM_Z}{\cos\theta_W} \left[ \left\{ \begin{array}{c} \cos^2\theta_\tau \\ \sin^2\theta_\tau \end{array} \right\} \left( \frac{1}{2} + e_\tau \sin^2\theta_W \right) + \left\{ \begin{array}{c} \sin^2\theta_\tau \\ \cos^2\theta_\tau \end{array} \right\} (e_\tau \sin^2\theta_W) \right], \quad (52e)$$

$$\left\{ \begin{array}{c} V(\mathcal{J}_\perp \tilde{\tau}_1 \tilde{\tau}_1) \\ V(\mathcal{J}_\perp \tilde{\tau}_2 \tilde{\tau}_2) \end{array} \right\} = -\frac{igm_\tau^2}{M_W^2} \tan\beta \mp \frac{igm_\tau}{2M_W} \sin 2\theta_\tau [A_\tau \tan\beta + \mu], \quad (52f)$$

where  $e_t$ ,  $e_b$ , and  $e_\tau$  are the electromagnetic charges  $2/3$ ,  $-1/3$ , and  $-1$  respectively. Notice that the D-terms do not contribute to the coupling of  $\mathcal{J}_\perp$  to the squarks. The mixed couplings (e.g.  $V(\mathcal{J} \tilde{t}_1 \tilde{t}_2)$ ) obviously do not contribute to the tadpole. Calculating the tadpole, and making use of the relations

$$\sin 2\theta_t = \frac{2m_{\tilde{t}_{LR}}^2}{m_{\tilde{t}_1}^2 - m_{\tilde{t}_2}^2} = \frac{2m_t(A_t + \mu \cot\beta)}{m_{\tilde{t}_1}^2 - m_{\tilde{t}_2}^2}, \quad (53a)$$

$$\cos 2\theta_t = \frac{m_{\tilde{t}_L}^2 - m_{\tilde{t}_R}^2}{m_{\tilde{t}_1}^2 - m_{\tilde{t}_2}^2} = \frac{(M_{Q_L}^2 - M_{t_R}^2) + \frac{1}{6} \cos 2\beta (8M_W^2 - 5M_Z^2)}{m_{\tilde{t}_1}^2 - m_{\tilde{t}_2}^2}, \quad (53b)$$

$$\sin 2\theta_b = \frac{2m_{\tilde{b}_{LR}}^2}{m_{\tilde{b}_1}^2 - m_{\tilde{b}_2}^2} = \frac{2m_b(A_b + \mu \tan\beta)}{m_{\tilde{b}_1}^2 - m_{\tilde{b}_2}^2}, \quad (53c)$$

$$\cos 2\theta_b = \frac{m_{\tilde{b}_L}^2 - m_{\tilde{b}_R}^2}{m_{\tilde{b}_1}^2 - m_{\tilde{b}_2}^2} = \frac{(M_{Q_L}^2 - M_{b_R}^2) - \frac{1}{6} \cos 2\beta (4M_W^2 - M_Z^2)}{m_{\tilde{b}_1}^2 - m_{\tilde{b}_2}^2}, \quad (53d)$$

$$\sin 2\theta_\tau = \frac{2m_{\tilde{\tau}_{LR}}^2}{m_{\tilde{\tau}_1}^2 - m_{\tilde{\tau}_2}^2} = \frac{2m_\tau(A_\tau + \mu \tan\beta)}{m_{\tilde{\tau}_1}^2 - m_{\tilde{\tau}_2}^2}, \quad (53e)$$

$$\cos 2\theta_\tau = \frac{m_{\tilde{\tau}_L}^2 - m_{\tilde{\tau}_R}^2}{m_{\tilde{\tau}_1}^2 - m_{\tilde{\tau}_2}^2} = \frac{(M_{L_L}^2 - M_{\tau_R}^2) - \frac{1}{2} \cos 2\beta (4M_W^2 - 3M_Z^2)}{m_{\tilde{\tau}_1}^2 - m_{\tilde{\tau}_2}^2}, \quad (53f)$$

one arrives at the top and bottom quark-squark contribution to the minimization conditions:

$$\begin{aligned} \Delta T_1^{(q)} &= \frac{3}{4\pi^2 v} \left[ m_t^4 \left( \ln \frac{m_t^2}{Q^2} - 1 \right) - m_b^4 \left( \ln \frac{m_b^2}{Q^2} - 1 \right) \right] \\ &+ \frac{3}{16\pi^2 v} \left\{ m_{\tilde{t}_{1,2}}^2 \left( \ln \frac{m_{\tilde{t}_{1,2}}^2}{Q^2} - 1 \right) \left[ -2m_t^2 + \frac{1}{2} M_Z^2 \right. \right. \right. \\ &\pm \frac{1}{m_{\tilde{t}_1}^2 - m_{\tilde{t}_2}^2} \left[ \frac{1}{3} (8M_W^2 - 5M_Z^2) \left[ \frac{1}{2} (M_{Q_L}^2 - M_{t_R}^2) + \frac{1}{12} \cos 2\beta (8M_W^2 - 5M_Z^2) \right] \right. \right. \\ &\left. \left. \left. + 2m_t^2 \left( (\mu \cot\beta)^2 - A_t^2 \right) \right] \right. \right. \\ &\left. \left. - m_{\tilde{b}_{1,2}}^2 \left( \ln \frac{m_{\tilde{b}_{1,2}}^2}{Q^2} - 1 \right) \left[ -2m_b^2 + \frac{1}{2} M_Z^2 \right] \right\} \end{aligned}$$

$$\begin{aligned} & \pm \frac{1}{m_{b_1}^2 - m_{b_2}^2} \left[ \frac{1}{3} (4M_W^2 - M_Z^2) \left[ \frac{1}{2} (M_{Q_L}^2 - M_{b_R}^2) - \frac{1}{12} \cos 2\beta (4M_W^2 - M_Z^2) \right] \right. \\ & \left. + 2m_b^2 \left( (\mu \tan \beta)^2 - A_b^2 \right) \right] \Bigg\}, \end{aligned} \quad (54a)$$

$$\begin{aligned} \Delta T_2^{(q)} &= -\frac{3}{4\pi^2 v} \left[ m_t^4 \left( \ln \frac{m_t^2}{Q^2} - 1 \right) \cot \beta + m_b^4 \left( \ln \frac{m_b^2}{Q^2} - 1 \right) \tan \beta \right] \\ &+ \frac{3}{8\pi^2 v} \left\{ m_{t_{1,2}}^2 \left( \ln \frac{m_{t_{1,2}}^2}{Q^2} - 1 \right) \cot \beta \left[ m_t^2 \pm \frac{1}{m_{t_1}^2 - m_{t_2}^2} m_t^2 (A_t + \mu \cot \beta) (A_t + \mu \tan \beta) \right] \right. \\ &\left. + m_{b_{1,2}}^2 \left( \ln \frac{m_{b_{1,2}}^2}{Q^2} - 1 \right) \tan \beta \left[ m_b^2 \pm \frac{1}{m_{b_1}^2 - m_{b_2}^2} m_b^2 (A_b + \mu \cot \beta) (A_b + \mu \tan \beta) \right] \right\}. \end{aligned} \quad (54b)$$

Also the tau lepton-slepton and sneutrino contributions are

$$\begin{aligned} \Delta T_1^{(l)} &= \frac{1}{4\pi^2 v} \left[ -m_\tau^4 \left( \ln \frac{m_\tau^2}{Q^2} - 1 \right) \right. \\ &+ \frac{1}{16\pi^2 v} \left\{ m_{\tilde{\nu}}^2 M_Z^2 \left( \ln \frac{m_{\tilde{\nu}}^2}{Q^2} - 1 \right) \right. \\ &\left. - m_{\tilde{\tau}_{1,2}}^2 \left( \ln \frac{m_{\tilde{\tau}_{1,2}}^2}{Q^2} - 1 \right) \left[ -2m_\tau^2 + \frac{1}{2} M_Z^2 \right] \right. \\ &\left. \pm \frac{1}{m_{\tilde{\tau}_1}^2 - m_{\tilde{\tau}_2}^2} \left[ (4M_W^2 - 3M_Z^2) \left[ \frac{1}{2} (M_{L_L}^2 - M_{\tau_R}^2) - \frac{1}{4} \cos 2\beta (4M_W^2 - 3M_Z^2) \right] \right. \right. \\ &\left. \left. + 2m_\tau^2 \left( (\mu \tan \beta)^2 - A_\tau^2 \right) \right] \right\}, \end{aligned} \quad (55a)$$

$$\begin{aligned} \Delta T_2^{(l)} &= -\frac{1}{4\pi^2 v} \left[ m_\tau^4 \left( \ln \frac{m_\tau^2}{Q^2} - 1 \right) \tan \beta \right] + \frac{1}{8\pi^2 v} \left\{ m_{\tilde{\tau}_{1,2}}^2 \left( \ln \frac{m_{\tilde{\tau}_{1,2}}^2}{Q^2} - 1 \right) \tan \beta \right. \\ &\left. \times \left[ m_\tau^2 \pm \frac{1}{m_{\tilde{\tau}_1}^2 - m_{\tilde{\tau}_2}^2} m_\tau^2 (A_\tau + \mu \cot \beta) (A_\tau + \mu \tan \beta) \right] \right\}, \end{aligned} \quad (55b)$$

There are similar contributions from the first and second generations. Most of these terms in  $\Delta T_1$  and all of the terms in  $\Delta T_2$  are proportional to some powers of the quark or lepton mass, which is negligible in the light generations. However, there exist contributions to  $\Delta T_1$  which are proportional to  $M_Z^2$  and  $M_W^2$ ; these are zero only in the limit in which the squarks (or sleptons) are degenerate within each generation. This is not necessarily a good approximation; we find that the light squark/slepton contribution can be larger than the gauge boson contribution (see below), especially for moderate or large values of  $m_0$  and  $m_{\frac{1}{2}}$ . It is therefore important to include the light squarks and sleptons in a full one-loop analysis. Explicitly, the light squark and slepton contribution is

$$\begin{aligned} \Delta T_1^{(lq)} &= \frac{(2)3}{16\pi^2 v} \left\{ m_{\tilde{u}_{1,2}}^2 \left( \ln \frac{m_{\tilde{u}_{1,2}}^2}{Q^2} - 1 \right) \left[ \frac{1}{2} M_Z^2 \pm \left( \frac{1}{2} \right) \frac{1}{3} (8M_W^2 - 5M_Z^2) \right] \right. \\ &\left. - m_{\tilde{d}_{1,2}}^2 \left( \ln \frac{m_{\tilde{d}_{1,2}}^2}{Q^2} - 1 \right) \left[ \frac{1}{2} M_Z^2 \pm \left( \frac{1}{2} \right) \frac{1}{3} (4M_W^2 - M_Z^2) \right] \right\}, \end{aligned} \quad (56a)$$

$$\Delta T_1^{(ll)} = \frac{(2)1}{16\pi^2 v} \left\{ m_{\bar{\nu}}^2 \left( \ln \frac{m_{\bar{\nu}}^2}{Q^2} - 1 \right) \left[ M_Z^2 \right] - m_{\bar{e}_{1,2}}^2 \left( \ln \frac{m_{\bar{e}_{1,2}}^2}{Q^2} - 1 \right) \left[ \frac{1}{2} M_Z^2 \pm \left( \frac{1}{2} \right) (4M_W^2 - 3M_Z^2) \right] \right\}, \quad (56b)$$

$$\Delta T_2^{(lq)} = 0, \Delta T_2^{(ll)} = 0, \quad (56c)$$

where the factor of two includes both light generations.

If we neglect the contribution from the bottom quark and from the D-term contributions to the squark masses and couplings, the equations above reduce to

$$\Delta T_1^{(q)} = \frac{3m_t^2}{8\pi^2 v} \left[ 2f(m_t^2) - f(m_{\bar{t}_1}^2) - f(m_{\bar{t}_2}^2) + \frac{f(m_{\bar{t}_1}^2) - f(m_{\bar{t}_2}^2)}{m_{\bar{t}_1}^2 - m_{\bar{t}_2}^2} \left( (\mu \cot \beta)^2 - A_t^2 \right) \right], \quad (57a)$$

$$\Delta T_2^{(q)} = -\frac{3m_t^2 \cot \beta}{8\pi^2 v} \left[ 2f(m_t^2) - f(m_{\bar{t}_1}^2) - f(m_{\bar{t}_2}^2) - \frac{f(m_{\bar{t}_1}^2) - f(m_{\bar{t}_2}^2)}{m_{\bar{t}_1}^2 - m_{\bar{t}_2}^2} (A_t + \mu \cot \beta)(A_t + \mu \tan \beta) \right], \quad (57b)$$

where

$$f(m^2) = m^2 \left( \ln \frac{m^2}{Q^2} - 1 \right). \quad (58)$$

The neutralino mass matrix is

$$M_N = \begin{pmatrix} M_1 & 0 & -M_Z \cos \beta \sin \theta_W & M_Z \sin \beta \sin \theta_W \\ 0 & M_2 & M_Z \cos \beta \cos \theta_W & -M_Z \sin \beta \cos \theta_W \\ -M_Z \cos \beta \sin \theta_W & M_Z \cos \beta \cos \theta_W & 0 & \mu \\ M_Z \sin \beta \sin \theta_W & -M_Z \sin \beta \cos \theta_W & \mu & 0 \end{pmatrix}. \quad (59)$$

This mass matrix is symmetric and can be diagonalized by a single matrix  $Z$  as[58]

$$Z^* M_N Z^{-1}, \quad (60)$$

We choose  $Z$  to be a real matrix; then the diagonalized neutrino mass matrix can have negative entries. We let the entries be  $\epsilon_i M_{\chi_i^0}$  where  $M_{\chi_i^0}$  are *positive* masses and  $\epsilon_i$  takes on a value of +1 or -1. The diagonalization can be done numerically, or one can use the analytic expressions[59]

$$\epsilon_1 M_{\chi_1^0} = -\left(\frac{1}{2}a - \frac{1}{6}C_2\right)^{1/2} + \left[-\frac{1}{2}a - \frac{1}{3}C_2 + \frac{C_3}{(8a - \frac{8}{3}C_2)^{1/2}}\right]^{1/2} + \frac{1}{4}(M_1 + M_2), \quad (61a)$$

$$\epsilon_2 M_{\chi_2^0} = +\left(\frac{1}{2}a - \frac{1}{6}C_2\right)^{1/2} - \left[-\frac{1}{2}a - \frac{1}{3}C_2 - \frac{C_3}{(8a - \frac{8}{3}C_2)^{1/2}}\right]^{1/2} + \frac{1}{4}(M_1 + M_2), \quad (61b)$$

$$\epsilon_3 M_{\chi_3^0} = -\left(\frac{1}{2}a - \frac{1}{6}C_2\right)^{1/2} - \left[-\frac{1}{2}a - \frac{1}{3}C_2 + \frac{C_3}{(8a - \frac{8}{3}C_2)^{1/2}}\right]^{1/2} + \frac{1}{4}(M_1 + M_2), \quad (61c)$$

$$\epsilon_4 M_{\chi_4^0} = +\left(\frac{1}{2}a - \frac{1}{6}C_2\right)^{1/2} + \left[-\frac{1}{2}a - \frac{1}{3}C_2 - \frac{C_3}{(8a - \frac{8}{3}C_2)^{1/2}}\right]^{1/2} + \frac{1}{4}(M_1 + M_2), \quad (61d)$$

where

$$C_2 = (M_1 M_2 - M_Z^2 - \mu^2) - \frac{3}{8}(M_1 + M_2)^2, \quad (62a)$$

$$C_3 = -\frac{1}{8}(M_1 + M_2)^3 + \frac{1}{2}(M_1 + M_2)(M_1 M_2 - M_Z^2 - \mu^2) + (M_1 + M_2)\mu^2 \\ + (M_1 \cos^2 \theta_W + M_2 \sin^2 \theta_W)M_Z^2 + \mu M_Z^2 \sin 2\beta, \quad (62b)$$

$$C_4 = -(M_1 \cos^2 \theta_W + M_2 \sin^2 \theta_W)M_Z^2 \mu \sin 2\beta - M_1 M_2 \mu^2 \\ + \frac{1}{4}(M_1 + M_2)[(M_1 + M_2)\mu^2 + (M_1 \cos^2 \theta_W + M_2 \sin^2 \theta_W)M_Z^2 + \mu M_Z^2 \sin 2\beta] \\ + \frac{1}{16}(M_1 M_2 - M_Z^2 - \mu^2)(M_1 + M_2)^2 - \frac{3}{256}(M_1 + M_2)^4, \quad (62c)$$

$$a = \frac{1}{2^{1/3}} \text{Re} \left[ -S + i(D/27)^{1/2} \right]^{1/3}, \quad (62d)$$

$$D = -4U^3 - 27S^2, \quad U = -\frac{1}{3}C_2^2 - 4C_4, \quad S = -C_3^2 - \frac{2}{27}C_2^3 + \frac{8}{3}C_2 C_4. \quad (62e)$$

These masses given by the above expression are not necessarily such that  $M_{\chi_1^0} < M_{\chi_2^0} < M_{\chi_3^0} < M_{\chi_4^0}$ , but the eigenstates can be relabeled. We have corrected a typographical error in the definition of  $U$  given in Ref. [59]. The contribution to the minimization conditions is

$$\Delta T_1(\chi^0) = -\frac{1}{2} \sum_{i=1}^4 \frac{gM_{\chi_i^0}^3}{4\pi^2} \left[ Q''_{ii} \cos \beta + S''_{ii} \sin \beta \right] \left( \ln \frac{M_{\chi_i^0}^2}{Q^2} - 1 \right), \quad (63a)$$

$$\Delta T_2(\chi^0) = -\frac{1}{2} \sum_{i=1}^4 \frac{gM_{\chi_i^0}^3}{4\pi^2} \left[ Q''_{ii} \sin \beta - S''_{ii} \cos \beta \right] \left( \ln \frac{M_{\chi_i^0}^2}{Q^2} - 1 \right). \quad (63b)$$

The factors  $Q''_{ii}$  and  $S''_{ii}$  are defined as[60]

$$Q''_{ii} = [Z_{i3}(Z_{i2} - Z_{i1} \tan \theta_w)] \epsilon_i, \quad (64a)$$

$$S''_{ii} = [Z_{i4}(Z_{i2} - Z_{i1} \tan \theta_w)] \epsilon_i, \quad (64b)$$

where  $\epsilon_i$  is the sign of the  $i$ th eigenvalue of the neutralino mass matrix. The mixing matrix  $Z$  can also be given by analytic expressions[59]

$$\frac{Z_{i2}}{Z_{i1}} = -\frac{1}{\tan \theta_W} \frac{M_1 - \epsilon_i M_{\chi_i^0}}{M_2 - \epsilon_i M_{\chi_i^0}}, \quad (65a)$$

$$\frac{Z_{i3}}{Z_{i1}} = \frac{-\mu[M_2 - \epsilon_i M_{\chi_i^0}][M_1 - \epsilon_i M_{\chi_i^0}] - M_Z^2 \sin \beta \cos \beta [(M_1 - M_2) \cos^2 \theta_W + M_2 - \epsilon_i M_{\chi_i^0}]}{M_Z[M_2 - \epsilon_i M_{\chi_i^0}] \sin \theta_W [-\mu \cos \beta + \epsilon_i M_{\chi_i^0} \sin \beta]}, \quad (65b)$$

$$\frac{Z_{i4}}{Z_{i1}} = \frac{-\epsilon_i M_{\chi_i^0} [M_2 - \epsilon_i M_{\chi_i^0}] [M_1 - \epsilon_i M_{\chi_i^0}] - M_Z^2 \cos^2 \beta [(M_1 - M_2) \cos^2 \theta_W + M_2 - \epsilon_i M_{\chi_i^0}]}{M_Z[M_2 - \epsilon_i M_{\chi_i^0}] \sin \theta_W [-\mu \cos \beta + \epsilon_i M_{\chi_i^0} \sin \beta]}, \quad (65c)$$

and

$$Z_{i1} = \left[ 1 + \left( \frac{Z_{i2}}{Z_{i1}} \right)^2 + \left( \frac{Z_{i3}}{Z_{i1}} \right)^2 + \left( \frac{Z_{i4}}{Z_{i1}} \right)^2 \right]^{-1/2}. \quad (66)$$

In terms of the mixing matrix  $Z$  the bino and gaugino purities are defined as

$$B_P = Z_{11}^2, \quad (67a)$$

$$G_P = Z_{11}^2 + Z_{12}^2, \quad (67b)$$



respectively.

The chargino mass matrix is

$$M_C = \begin{pmatrix} M_2 & \sqrt{2}M_W \sin \beta \\ \sqrt{2}M_W \cos \beta & -\mu \end{pmatrix}. \quad (68)$$

This mass matrix is not symmetric and must be diagonalized by two matrices  $U$  and  $V$  as[58]

$$U^* M_C V^{-1}, \quad (69)$$

where

$$U = O_-, \quad V = \begin{cases} O_+ & , \det X \geq 0 \\ \sigma_3 O_+ & , \det X < 0 \end{cases}, \quad O_{\pm} = \begin{pmatrix} \cos \phi_{\pm} & \sin \phi_{\pm} \\ -\sin \phi_{\pm} & \cos \phi_{\pm} \end{pmatrix}. \quad (70)$$

Here  $\sigma_3$  is the Pauli matrix, and

$$\tan 2\phi_- = 2\sqrt{2}M_W \frac{-\mu \sin \beta + M_2 \cos \beta}{M_2^2 - \mu^2 - 2M_W^2 \cos 2\beta}, \quad (71)$$

$$\tan 2\phi_+ = 2\sqrt{2}M_W \frac{-\mu \cos \beta + M_2 \sin \beta}{M_2^2 - \mu^2 + 2M_W^2 \cos 2\beta}. \quad (72)$$

The chargino masses are

$$M_{\chi^{\pm}}^2 = \frac{1}{2} \left[ M_2^2 + \mu^2 + 2M_W^2 \pm [(M_2^2 - \mu^2)^2 + 4M_W^4 \cos^2 2\beta + 4M_W^2 (M_2^2 + \mu^2 - 2M_2\mu \sin 2\beta)]^{1/2} \right]. \quad (73)$$

The contribution to the minimization conditions is

$$\Delta T_1^{(\chi^{\pm})} = - \sum_{i=1}^2 \frac{gM_{\chi_i^{\pm}}^3}{4\pi^2} \left[ Q_{ii} \cos \beta - S_{ii} \sin \beta \right] \left( \ln \frac{M_{\chi_i^{\pm}}^2}{Q^2} - 1 \right), \quad (74a)$$

$$\Delta T_2^{(\chi^{\pm})} = - \sum_{i=1}^2 \frac{gM_{\chi_i^{\pm}}^3}{4\pi^2} \left[ Q_{ii} \sin \beta + S_{ii} \cos \beta \right] \left( \ln \frac{M_{\chi_i^{\pm}}^2}{Q^2} - 1 \right). \quad (74b)$$

The factors  $Q_{ii}$  and  $S_{ii}$  are defined as

$$Q_{ii} = \sqrt{\frac{1}{2}} V_{i1} U_{i2}, \quad (75a)$$

$$S_{ii} = \sqrt{\frac{1}{2}} V_{i2} U_{i1}. \quad (75b)$$

The Higgs bosons and Goldstone bosons contribute the following contributions in the Landau gauge

$$\begin{aligned} \Delta T_1^{(H)} &= \frac{gM_{H^{\pm}}^2}{32\pi^2} \left( 2M_W - \frac{M_Z}{\cos \theta_w} \right) \cos 2\beta \left( \ln \frac{M_{H^{\pm}}^2}{Q^2} - 1 \right) \\ &+ \frac{gM_Z M_h^2}{64\pi^2 \cos \theta_w} (-2 \cos 2\alpha + \cos 2\beta) \left( \ln \frac{M_h^2}{Q^2} - 1 \right) \end{aligned}$$

$$\begin{aligned}
& + \frac{gM_Z M_H^2}{64\pi^2 \cos \theta_w} (2 \cos 2\alpha + \cos 2\beta) \left( \ln \frac{M_H^2}{Q^2} - 1 \right) \\
& - \frac{gM_Z M_A^2}{64\pi^2 \cos \theta_w} \cos 2\beta \left( \ln \frac{M_A^2}{Q^2} - 1 \right), \tag{76a}
\end{aligned}$$

$$\begin{aligned}
\Delta T_2^{(H)} & = \frac{gM_W M_{H^\pm}^2}{16\pi^2} \sin 2\beta \left( \ln \frac{M_{H^\pm}^2}{Q^2} - 1 \right) \\
& + \frac{gM_Z M_h^2}{64\pi^2 \cos \theta_w} (\sin 2\alpha + \sin 2\beta) \left( \ln \frac{M_h^2}{Q^2} - 1 \right) \\
& + \frac{gM_Z M_H^2}{64\pi^2 \cos \theta_w} (-\sin 2\alpha + \sin 2\beta) \left( \ln \frac{M_H^2}{Q^2} - 1 \right). \tag{76b}
\end{aligned}$$

The angle factor  $\alpha$  can be eliminated in the above equations using the tree level relations for the Higgs masses:

$$-2 \cos 2\alpha + \cos 2\beta = \cos 2\beta \left( \frac{3M_H^2 + M_h^2 - 4M_Z^2}{M_H^2 - M_h^2} \right), \tag{77a}$$

$$2 \cos 2\alpha + \cos 2\beta = \cos 2\beta \left( \frac{3M_h^2 + M_H^2 - 4M_Z^2}{M_h^2 - M_H^2} \right), \tag{77b}$$

$$\sin 2\alpha + \sin 2\beta = \sin 2\beta \left( \frac{2M_h^2}{M_h^2 - M_H^2} \right), \tag{77c}$$

$$-\sin 2\alpha + \sin 2\beta = \sin 2\beta \left( \frac{2M_H^2}{M_H^2 - M_h^2} \right). \tag{77d}$$

The gauge boson contribution is

$$\begin{aligned}
\Delta T_1^{(GB)} & = \frac{3gM_W^3}{16\pi^2} \cos 2\beta \left( \ln \frac{M_W^2}{Q^2} - 1 \right) \\
& + \frac{3gM_Z^3}{32\pi^2 \cos \theta_w} \cos 2\beta \left( \ln \frac{M_Z^2}{Q^2} - 1 \right), \tag{78a}
\end{aligned}$$

$$\begin{aligned}
\Delta T_2^{(GB)} & = \frac{3gM_W^3}{16\pi^2} \sin 2\beta \left( \ln \frac{M_W^2}{Q^2} - 1 \right) \\
& + \frac{3gM_Z^3}{32\pi^2 \cos \theta_w} \sin 2\beta \left( \ln \frac{M_Z^2}{Q^2} - 1 \right). \tag{78b}
\end{aligned}$$

Then the minimization conditions at one-loop are the following:

$$T_1 + \sum_i \Delta T_1^{(i)} = 0, \tag{79a}$$

$$T_2 + \sum_i \Delta T_2^{(i)} = 0, \tag{79b}$$

where  $i = q, l, lq, ll, \chi^0, \chi^\pm, H, GB$ .

## References

- [1] For reviews see J. Wess and J. Bagger, ‘‘Supersymmetry and Supergravity,’’ Princeton University Press (1983); P. Fayet and S. Ferrara, Phys. Rep. **C32**, 249

- (1977); P. van Nieuwenhuizen, Phys. Rep. **C68**, 189 (1981); H. P. Nilles, Phys. Rep. **C110**, 1 (1984); H. Haber and G. Kane, Phys. Rep. **C117**, 75 (1985); M. F. Sohnius, Phys. Rep. **C128**, 39 (1985); X. Tata, Lectures presented at Mt. Sorak Symp. on the Standard and Beyond, Mt. Sorak, Korea, Aug 1990; 20 Years of Supersymmetry Conference (1993); SUSY-93 Conference Northeastern University (1993); J. Lopez, Texas A&M preprint CTP-TAMU-42/93 from the Proceedings of the International School of Subnuclear Physics 31st Course, Erice, Italy; D. R. T. Jones, TASI-93 Lectures, Boulder, Co (1993).
- [2] U. Amaldi, W. de Boer, and H. Furstenau, Phys. Lett. **B260**, 447 (1991); J. Ellis, S. Kelley and D. V. Nanopoulos, Phys. Lett. **B260** 131 (1991); P. Langacker and M. Luo, Phys. Rev. **D44**, 817 (1991).
- [3] M. Chanowitz, J. Ellis and M. Gaillard, Nucl. Phys. **128**, 506 (1977).
- [4] For a review see P. Nath, R. Arnowitt, and A. H. Chamseddine, “Applied  $N = 1$  Supergravity,” World Scientific (1984).
- [5] L. E. Ibañez and G. G. Ross, Phys. Lett. **B110**, 215 (1982); L. Alvarez-Gaumé, M. Claudson and M. B. Wise, Nucl. Phys. **207**, 96 (1982); J. Ellis, D. V. Nanopoulos, and K. Tamvakis, Phys. Lett. **B121**, 123 (1983); L. E. Ibañez, Nucl. Phys. **218**, 514 (1983); L. Alvarez-Gaumé, J. Polchinski and M. B. Wise, Nucl. Phys. **221**, 495 (1983); J. Ellis, J. S. Hagelin, D. V. Nanopoulos, and K. Tamvakis, Phys. Lett. **B125**, 275 (1983); L. E. Ibañez and C. Lopez, Phys. Lett. **B126**, 54 (1983); Nucl. Phys. **B233**, 511 (1984); C. Kounnas, A. B. Lahanas, D. V. Nanopoulos, and M. Quiros, Nucl. Phys. **B236**, 438 (1984); U. Ellwanger, Nucl. Phys. **B238**, 665 (1984); L. E. Ibañez, C. Lopez, and C. Muñoz, Nucl. Phys. **B256**, 218 (1985); A. Bouquet, J. Kaplan, and C. A. Savoy, Nucl. Phys. **B262**, 299 (1985); H. J. Kappen, Phys. Rev. **D35**, 3923 (1987); M. Drees, Phys. Rev. **D38**, 718 (1988); H. J. Kappen, Phys. Rev. **D38**, 721 (1988); B. Gato, Z. Phys. **C37**, 407 (1988); G. F. Giudice and G. Ridolfi, Z. Phys. **C41**, 447 (1988); S. P. Li and H. Navelet, Nucl. Phys. **B319**, 239 (1989).
- [6] G. Gamberini, G. Ridolfi, and F. Zwirner, Nucl. Phys. **B331**, 331 (1990).
- [7] R. Arnowitt and P. Nath, Phys. Rev. **69**, 725 (1992); Phys. Lett. **B289**, 368 (1992).
- [8] G. G. Ross and R. G. Roberts, Nucl. Phys. **B377**, 571 (1992).
- [9] S. Kelley, J. L. Lopez, D. V. Nanopoulos, H. Pois, and K. Yuan, Nucl. Phys. **B398**, 3 (1993).
- [10] M. Olechowski and S. Pokorski, Nucl. Phys. **B404**, 590 (1993).
- [11] P. Ramond, Institute for Fundamental Theory Preprint UFIFT-HEP-93-13 (1993); D. J. Castaño, E. J. Piard, and P. Ramond, Institute for Fundamental Theory Preprint UFIFT-HEP-93-18 (1993).

- [12] W. de Boer, R. Ehret, and D. I. Kazakov, Inst. für Experimentelle Kernphysik preprint IEKP-KA/93-13, Contribution to the International Symposium on Lepton Photon Interactions, Ithaca, NY (1993).
- [13] M. Carena, M. Olechowski, S. Pokorski, and C. E. M. Wagner, CERN preprint CERN-TH.7060/93 (1993).
- [14] B. Pendleton and G. G. Ross, Phys. Lett. **98B**, 291 (1981); C. T. Hill, Phys. Rev. **D24**, 691 (1981); W. Zimmermann, Commun. Math. Phys. **97**, 211 (1985); J. Kubo, K. Sibold, and W. Zimmerman, Phys. Lett. **B200**, 191 (1989); C. D. Froggatt, I. G. Knowles, and R. G. Moorhouse, Phys. Lett. **B249**, 273 (1990); **B298**, 356 (1993); M. Carena, T. E. Clark, C. E. M. Wagner, W. A. Bardeen, and K. Sasaki, Nucl. Phys. **B369**, 33 (1992).
- [15] V. Barger, M.S. Berger, and P. Ohmann, Phys. Rev. **D47**, 1093 (1993); *ibid.* **D47**, 2038 (1993); V. Barger, M.S. Berger, P. Ohmann, and R.J.N. Phillips, Phys. Lett. **B314**, 351 (1993).
- [16] M. Carena, S. Pokorski, and C. E. M. Wagner, Nucl. Phys. **B406**, 59 (1993).
- [17] P. Langacker and N. Polonsky, University of Pennsylvania preprint UPR-0556-T (1993); N. Polonsky, Talk presented at the XVI Kazimierz Meeting on Elementary Particle Physics, Kazimierz, Poland (1993).
- [18] W. Bardeen, M. Carena, S. Pokorski, and C. E. M. Wagner, Munich preprint MPI-Ph/93-58.
- [19] L. J. Hall in “Supersymmetry and Supergravity Nonperturbative QCD,” eds. P. Roy and V. Singh, Springer-Verlag, Berlin (1984).
- [20] V. Kaplunovsky and J. Louis, Nucl. Phys. **B306**, 269 (1993), and references therein.
- [21] A. Brignole, L. E. Ibáñez, and C. Muñoz, Dept. of Física Teórica preprint FTUAM-93/26.
- [22] G. F. Giudice and E. Roulet, Phys. Lett. **B315**, 107 (1993).
- [23] R. Tarrach, Nucl. Phys. **B183**, 384 (1981).
- [24] M. Diaz and H. Haber, Phys. Rev. **D46**, 3086 (1992).
- [25] W. Siegel, Phys. Lett. **B84**, 193 (1979); D. M. Capper D. R. T. Jones, and P. van Nieuwenhuizen, Nucl. Phys. **B167**, 479, (1980).
- [26] S. Weinberg, Phys. Rev. **D7**, 2887 (1973); S. Y. Lee and A. M. Sciaccaluga, Nucl. Phys. **B96**, 435 (1975); K. T. Mahanthappa and M. A. Sher, Phys. Rev. **D22**, 1711 (1980).

- [27] M. Sher, Phys. Rep. **C179**, 273 (1989).
- [28] J. L. Lopez, Texas A&M University preprint CTP-TAMU-42/93.
- [29] S. Coleman and E. Weinberg, Phys. Rev. **D7**, 1888 (1973).
- [30] A. B. Lahanas and D. V. Nanopoulos, Phys. Rep. **C145**, 1 (1987), and references therein.
- [31] R. Barbieri and G. F. Giudice, Nucl. Phys. **B306**, 63 (1993).
- [32] B. de Carlos and J. A. Casas, Phys. Lett. **B309**, 320 (1993); B. de Carlos, CERN preprint CERN-TH-7024-93, Talk given at XVI International Warsaw Meeting on Elementary Particle Physics (1993).
- [33] J. Ellis, A. B. Lahanas, D. V. Nanopoulos, and K. Tamvakis, Phys. Lett. **B134**, 129 (1984); J. Ellis, C. Kounnas, D. V. Nanopoulos, Nucl. Phys. **B241**, 406 (1984); Nucl. Phys. **B247**, 373 (1984).
- [34] R. Barbieri, J. Louis, and M. Moretti, CERN-TH.6856/93.
- [35] J. L. Lopez, D. V. Nanopolous, and A. Zichichi, CERN preprint CERN-TH.6926/93.
- [36] M. Olechowski and S. Pokorski, Phys. Lett. **B214**, 393 (1991); B. Ananthanarayan et al., Phys. Rev. **D44**, 1613 (1991); S. Kelley et al., Phys. Lett. **B274**, 387 (1992); B. Ananthanarayan, G. Lazarides, and Q. Shafi, Phys. Lett. **B300**, 245 (1993); G. Anderson, S. Dimopoulos, L. J. Hall, S. Raby, and G. D. Starkman, Lawrence Berkeley Laboratory preprint LBL-33531 (1993); B. Ananthanarayan and Q. Shafi, Bartol Research Institute preprint BA-93-25 (1993).
- [37] Particle Data Book, Phys. Rev. **D45** (1992).
- [38] J.-M. Frère, D. R. T. Jones, and S. Raby, Nucl. Phys. **B222**, 11 (1983); Y. Yamada, Phys. Lett. **B316**, 109 (1993); S. P. Martin and M. T. Vaughn, Northeastern University preprint NIB-3072-93TH.
- [39] R. Barbieri and L. J. Hall, Phys. Rev. Lett. **68**, 752 (1992).
- [40] P. Langacker and N. Polonsky, Phys. Rev. **D47**, 4028 (1993).
- [41] A. E. Faraggi, B. Grinstein, and S. Meshkov, Phys. Rev. **D47**, 5018 (1993).
- [42] K. Hagiwara and Y. Yamada, Phys. Rev. Lett. **70**, 709 (1993).
- [43] F. M. Borzumati, DESY preprint 93-090 (1993).
- [44] J. Ellis, G. Ridolfi, and F. Zwirner, Phys. Lett. **B262**, 477 (1991); A. Brignole, J. Ellis, G. Ridolfi, and F. Zwirner, Phys. Lett. **B271**, 123 (1991).

- [45] H. E. Haber and R. Hempfling, Phys. Rev. **D48**, 4280 (1993).
- [46] M. Drees and M. M. Nojiri, Phys. Rev. **D47**, 376 (1993).
- [47] S. Bertolini, F. Borzumati, A. Masiero, and G. Ridolfi, Nucl. Phys. **B353**, 591 (1993).
- [48] V. Barger, M. S. Berger, and R. J. N. Phillips, Phys. Rev. Lett. **70**, 1368 (1993); J. L. Hewett, Phys. Rev. Lett. **70**, 1045 (1993); M. A. Diaz, Phys. Lett. **B304**, 278 (1993); J. L. Lopez, D. V. Nanopoulos, and G. T. Park, Phys. Rev. **D48**, 974 (1993); Y. Grossman and Y. Nir, Phys. Lett. **B313**, 126 (1993); Y. Okada, Phys. Lett. **B315**, 119 (1993); R. Garisto and J. N. Ng, Phys. Lett. **B315**, 372 (1993); J. L. Lopez, D. V. Nanopoulos, G. T. Park, and A. Zichichi, Texas A&M preprint CTP-TAMU-40/93 (1993); G. Park, Texas A&M preprint CTP-TAMU-69/93 (1993); M. A. Diaz, Vanderbilt preprint VAND-TH-93-13 (1993).
- [49] V. Barger, M. S. Berger, P. Ohmann and R. J. N. Phillips, in preparation.
- [50] J. L. Lopez, D. V. Nanopoulos, and H. Pois Phys. Rev. **D47**, 2468 (1993).
- [51] J. L. Lopez, D. V. Nanopolous, H. Pois, X. Wang, and A. Zichichi, Phys. Lett. **B306**, 73 (1993).
- [52] For an overview of dark matter in these models, see e. g. J. L. Lopez, D. V. Nanopoulos, and K. Yuan, Nucl. Phys. **B370**, 445 (1992); S. Kelley, J. L. Lopez, D. V. Nanopoulos, H. Pois, and K. Yuan, Phys. Rev. **D47**, 2461 (1993); L. Roszkowski, University of Michigan preprint UM-TH-93-06 (1993).
- [53] R. G. Roberts and L. Roszkowski, Phys. Lett. **B309**, 329 (1993).
- [54] C. Alcock et al. (MACHO Collaboration), **Nature**, in press (1993).
- [55] E. Aubourg et al. (EROS Collaboration), **Nature**, in press (1993).
- [56] M. Turner, Fermilab preprint FNAL-Pub-93/298-A (1993).
- [57] K. Inoue, A. Kakuto, H. Komatsu and H. Takeshita, Prog. Theor. Phys. **68**, 927 (1982); **71**, 413 (1984).
- [58] H. Haber and G. Kane, Phys. Rep. **C117**, 75 (1985).
- [59] M. M. El Kheishen, A. A. Shafik, and A. A. Aboshousha, Phys. Rev. **D45**, 4345 (1992).
- [60] J.F. Gunion, H.E. Haber, G.L. Kane and S. Dawson, “The Higgs-Hunter’s Guide”, Addison-Wesley (1990).